AN ABSTRACT OF THE THESIS OF

GARY FRANCIS ROSSKNECHT (Name) for the MASTER OF SCIENCE (Degree)

in OCEANOGRAPHY (Major) presented on April 4, 1972 (Date)

Title: A STUDY OF AIRBORNE SEA-SALT PARTICLES IN WESTERN OREGON

Abstract approved: Redacted for privacy

Dr. William P. Elliott

The purpose of the study was to measure the number and mass of airborne sea-salt particles (ASSP) as a function of distance inland from the ocean at Newport, Oregon. Forty-nine measurements of ASSP were made on three separate days along a line extending from the beach at Newport, Oregon to a point 50 kilometers inland.

The number and total mass of ASSP was found to decrease very sharply in the first four kilometers from the beach and to decrease more gradually further inland. The observed inland distribution curves for the data of July 14, 1971 were fitted to the theoretical model presented by Tanaka (1966) for the inland distribution of giant ASSP. It was found for ASSP with equivalent dry diameters between 2.0 and 4.7μ that the model could be fitted quite well, but for ASSP smaller than 2μ the predicted values inland were too high.

The size distributions of ASSP samples taken at sea and greater then eight kilometers inland from the shoreline were well-described by an exponential random variable, but samples taken inland within eight kilometers of the shoreline exhibited a diameter distribution significantly different from an exponential.

A Study of Airborne Sea-Salt Particles in Western Oregon

by

Gary Francis Rossknecht

A THESIS

submitted to

Oregon State University

in partial fulfillment of
the requirements for the
degree of

Master of Science

June 1972

APPROVED:

Redacted for privacy

Associate Professor of Oceanography
in charge of major

Redacted for privacy

Chairman of Department of Oceanography

Redacted for privacy

Dean of Graduate School

Date thesis is presented April 4, 1972

Typed by Muriel Davis for Gary Francis Rossknecht

ACKNOWLEDGMENT

I would like to thank Dr. William P. Elliott, my major professor, for his support and guidance in this investigation. I want to thank Dr. Fred L. Ramsey for his help with the statistical analysis of the data. I would also like to acknowledge the assistance provided by Dick Egami and Dave Enfield.

This investigation was supported by the National Science Foundation Grants no. GA-1618 and GA-31141.

TABLE OF CONTENTS

LIST OF FIGURES

LIST OF TABLES

A STUDY OF AIRBORNE SEA-SALT PARTICLES IN WESTERN OREGON

I. INTRODUCTION

This study is concerned with the inland penetration of airborne sea-salt particles. Sea-salt particles originate as tiny droplets of sea water that are injected into the air when tiny bubbles rise to the sea surface and burst. These bubbles result mainly from breaking waves. In the atmosphere the sea-salt in the droplets is concentrated by evaporation of the droplet. The resulting tiny particles of sea-salt or droplets of concentrated salt solution are an important component of the natural aerosols found in the atmosphere.

It will be convenient to abbreviate the term airborne sea-salt particles by ASSP.

The importance of ASSP lies in the role they play in the formation of large cloud drops. Many workers, including Bowen (1950), Squires (1952), and Twomey (1955) have suggested that large hydroscopic particles such as ASSP, can produce a population of giant cloud droplets which are thought to be necessary for the production of rain in non-freezing clouds. Lodge (1955) said that large ASSP may become the large cloud droplets required for the production of rain from warm clouds. Woodcock (1952) has found that ASSP are present at cloud levels in marine air over land and that their number and size agree in part with the assumption that each salt particle becomes a raindrop.

Murty, Roy, and Kapoor (1965, p. 67) have said

> The study of aerosols in the "large" (radius < 1 micron) and "giant" (radius > 1 micron) size range is important on account of their widely accepted role in cloud and precipitation development.

The purpose of this study is to determine just how far inland from the coast of Oregon ASSP of the larger sizes can penetrate. This thesis describes the results of measurements made to determine the concentration and size distribution of ASSP with diameters greater than 1.24 micrometers (μ) as a function of distance from the ocean.

Chapter II examines the work of other investigators. Chapter III explains how the ASSP were detected and counted and gives an account of some problems of measurement that arose. The chapter on data presents the data and weather conditions at the time of sampling. The last two chapters report the data analysis and conclusions.

II. BACKGROUND

Physical Characteristics

ASSP are classified as "large" if they consist of a mass of salt that has an equivalent dry diameter of .2 to 2μ, and as "giant" if the dry diameter is 2 to 20μ (Junge, 1963). The mass of a 2 micrometer diameter ASSP is 8.8×10^{-12} gram.

Due to their hygroscopicity, ASSP are not always "dry." Rather they exist as saline droplets with a salinity that depends on the relative humidity. If we take a crystalline ASSP at a humidity of zero and slowly increase the humidity, we will observe a phase transition from solid to liquid and an accompanying increase in diameter at 73% relative humidity (Twomey, 1954). If we then lower the relative humidity, the reverse phase change will not occur until around 40% relative humidity (Junge, 1963). A considerable salt supersaturation can occur when the humidity is lowered (Junge, 1963). Figure 2.1 illustrates this phase transition process for a 2μ salt particle.

For this study we will use curve A in Figure 2.1 to determine the size and salinity of ASSP for a particular relative humidity and dry diameter. Humidity as low as 40% was not encountered in this study so the particles never had a chance to crystallize.

Curve A and similar curves for other size hygroscopic particles are referred to as Kohler curves (Fletcher, 1966). A Kohler curve

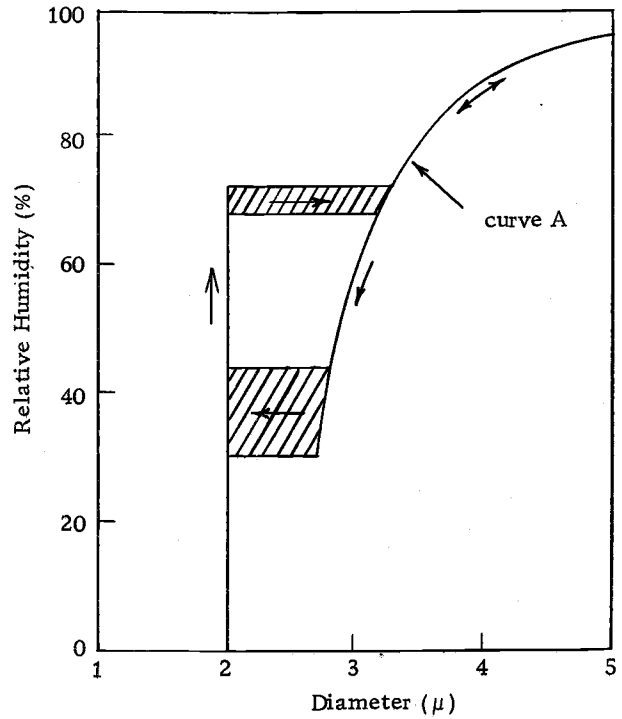

Figure 2.1. Phase-transition curve for a 2 μ ASSP (after Fletcher, 1966).

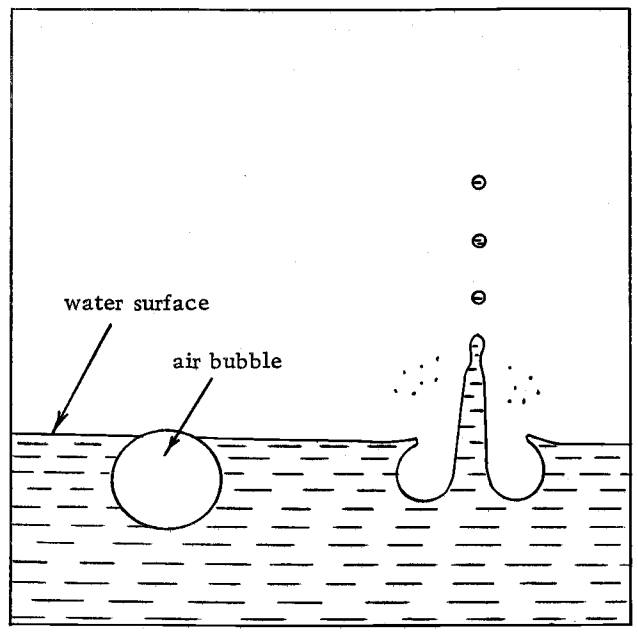

Figure 2.2. The formation of ASSP from a bursting air bubble (after Mason, 1962).

gives the equilibrium radius of a solution droplet as a function of saturation ratio (relative humidity) for a particular mass of salt. The curves are based on the balance that is achieved between the decreased vapor-pressure over an aqueous solution and the increased vapor-pressure caused by the surface curvature of small droplets (Fletcher, 1966). The effect of decreased vapor pressure due to an aqueous solution is expressed by Raoult's law:

$$\frac{P'}{P} = m \tag{2.1}$$

where P' is the vapor-pressure over a solution containing a mole fraction m of water and P is the vapor pressure over pure water. The Kelvin equation gives the ratio of the vapor pressure over a droplet of radius r to the vapor pressure over a flat surface:

$$\frac{P_r}{P_\infty} = \exp\left[\frac{2\sigma}{n_L kTr}\right] \tag{2.2}$$

σ is the surface-tension, n_L is the number of molecules per unit volume of liquid, k is the Boltzmann's constant, and T is the absolute temperature. Combining equations 2.1 and 2.2 we have for the water vapor-pressure over a solution droplet

$$\frac{P'_r}{P_\infty} = m \exp\left(\frac{2\sigma'}{n_L kTr}\right) \tag{2.3}$$

where the primed quantities refer to the solution at the concentration involved. m, the mole fraction of water is given by

$$(2.4) \qquad m = \left[1 + \frac{i b M_0}{M(4/3\,\pi r^3 \rho' - b)}\right]^{-1}$$

where i is the vant Hoff factor which takes account of the dissociation of inorganic salts, b is the mass of salt involved, M is the gram-molecular weight of the salt, M_0 is the gram-molecular weight of water and ρ' is the density of the droplet. A Kohler curve is a plot of the saturation ratio $\frac{P'_r}{P_\infty}$ versus r for a particular mass of salt.

The fall velocity of ASSP can be accurately determined from Stokes law for the terminal velocity of small spheres. The diameter and density of the ASSP will determine the fall velocity according to:

$$v_T = \frac{2gr}{9\eta}(\rho_2 - \rho_1)$$

g is the acceleration of gravity

r is the droplet radius

η is the coefficient of viscosity of air

ρ_2 is the droplet density

ρ_1 is the air density

ASSP with a diameter greater than 20 microns are seldom found because they fall to earth relatively fast: a 20μ ASSP would have a terminal velocity of about 3 cm/sec.

Production

Casually, one might think that ASSP would be the result of spray

and foam thrown high into the air during stormy sea conditions. Spray droplets produced in this way are usually much too large to remain airborne and they settle back to the surface. ASSP are produced by a more subtle process that occurs when small bubbles rise to the sea surface and burst.

The mechanism of production of ASSP from tiny bursting bubbles has been intensely studied by several investigators. Woodcock et al. (1953) made high speed motion pictures in the laboratory of bursting bubbles and found that the collapse of an air bubble when it reaches a water surface results in the formation of a tiny jet of water. This jet breaks into about five droplets which are projected upward to heights ranging from .5 to 15 cm. Figure 2.2 shows schematically how the bursting of a bubble creates a small jet which breaks up into droplets and ejects them upward. The energy for the jet formation is derived from the collapse of the bubble cavity.

Kientzler, et al. (1954) found that only very small bubbles are effective in producing droplets small enough to cause ASSP. Bubbles larger than 1.8mm diameter did not eject droplets of a size that could result in ASSP.

Moore and Mason (1954) investigated the size of the jet droplets produced by different size bubbles. Bubbles with diameters from .2 to 1.8 mm produced droplets with diameters that were about 1/10 the original bubble diameter. They also found evidence that the

disintegration of the bubble film produces many drops, each much smaller than those droplets produced by the liquid jet. Day (1964) investigated these film droplets with a cloud chamber and found that 300-400 film droplets were produced when the bubble film of a 4mm diameter bubble burst in sea water. The film droplets, however, produce much smaller particles known as condensation nuclei, in a size range not covered in this thesis. It is the droplets in the central jet that result in ASSP with diameters >1μ.

Bubbles which are of a size that produce ASSP result from the breaking of waves. Air is captured by the collapsing wavecrests and rises to the sea surface in the form of tiny bubbles. All forms of precipitation and also effective bubble producers (Roll, 1965). Horne (1966) has suggested that some bubbles appear to result from the growth of microbubbles of gas already existing in the water column.

The rate of production of ASSP with diameters greater than .2μ was investigated by Moore and Mason (1954). They estimate the maximum production rate (encountered only when the sea is extremely agitated) to be 100 particles per square cm per second. Blanchard and Woodcock (1957) estimated a production rate of 34 $cm^{-2} sec^{-1}$ for a less agitated sea condition.

Composition

The relative composition of the particles sampled in this study is assumed to be that of standard sea water for the major components. This assumption is generally valid for giant ASSP. Junge (1956) found the Cl/Na ratio of ASSP in maritime air was the same as sea water within the limits of accuracy of the technique. Twomey (1954) used a phase transition method to determine the relative composition of hygroscopic particles in the atmosphere over New South Wales. He found the great majority of giant hygroscopic particles were composed of sea-salt, sometimes in combination with insoluble material. Woodcock and Gifford (1949) sampled ASSP over the ocean and found that the particles had the relative composition of sea salt within the accuracy of the method used.

Size Distribution

A size distribution as used here is a graph or formula that shows the relative number of particles of different sizes. The particle size can be expressed by its diameter, mass, surface area, or volume. The distribution of particle diameters will be discussed here. Mass, surface area, or volume distribution can be determined once diameter distribution is known.

An examination of the previous work on diameter distributions

of ASSP reveals that the exact shape of the distribution is not agreed upon by all investigators. Woodcock (1950, 1952, 1953, 1959) has made many quantitative determinations of the diameter distribution of ASSP. He does not, however, suggest any mathematical formulas to describe the distributions that he found. He presents graphs of the size distribution data and in some cases draws a smooth curve through the data. Figure 2.3 is an example of some of Woodcock's (1953) data.

Twomey (1955) and Lodge (1955) measured the size distribution of ASSP in Australia and Puerto Rico respectively. Both reported the size distributions found were similar to those found by Woodcock.

Junge (1953) suggested that continental aerosols of the large and giant class follow a number distribution law of the form $n(r) \propto r^{-\beta}$ where $2 < \beta < 4$. Eriksson (1959) pointed out that Junge's power law ($kr^{-\beta}$) could not properly describe diameter distributions of ASSP. Junge (1963) said the size distribution for aerosols over the ocean is fundamentally different from that over continents.

Eriksson (1959) examined Woodcock's Hawaii (1957) data and averaged the 67 samples there to arrive at an average size distribution. He found that the number distribution thus obtained could be expressed by a function $\bar{n}(r) = Ae^{-b\sqrt{r}}$, where $\bar{n}(r)$ is the number density averaged over 67 samples, r is particle radius, and

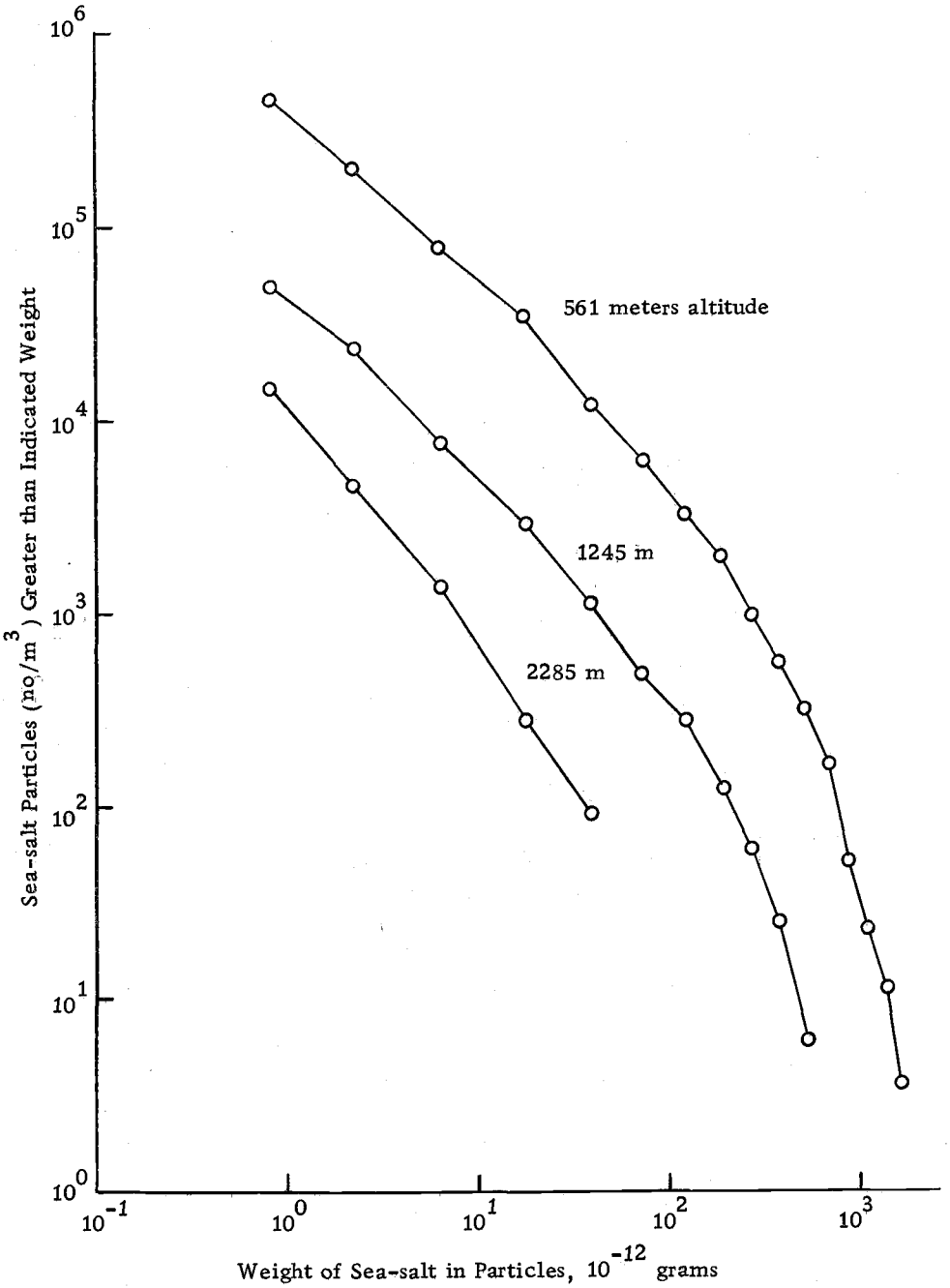

Figure 2.3. Example of Woodcock's ASSP size distribution data from over the Pacific near Hawaii, June 1951 (after Woodcock, 1953).

A and b are constants.

This writer has also examined Woodcock's (1957) data and confirmed the good fit of the data to the size distribution curve Eriksson has suggested. However, Eriksson's method of averaging Woodcock's ASSP distributions does not necessarily preserve the shape of the size distribution of individual samples. If each of the individual samples showed a number distribution of the form $n(r) = Ae^{-b\sqrt{r}}$ and each had a different characteristic A and b (which they must have from examining the data), then the averages of the concentrations in each diameter interval would not necessarily be of the form $e^{-b\sqrt{r}}$.

Inland Penetration

Twomey (1955) made a series of flights over southeastern Australia to measure the inland profile of ASSP with diameters greater than 4.5μ.

He took air samples at altitudes of 700 to 2700 meters, starting at the coast and following an air mass movement inland. Surprisingly, he found little correlation between the concentration of ASSP and length of trajectory over land. Samples taken inland frequently contained more sea-salt particles than samples at the coast.

Lodge (1955) took surface measurements of sea-salt particles with diameters greater than 3μ along an inland route in Puerto Rico near Ponce. The wind was onshore about 7-10 knots and five stations

were sampled over a distance of 80 miles. Lodge found a sharp decrease of ASSP numbers in the first 1/4 mile from the beach and a continuing lesser decrease to 80 miles inland. The rate of decrease with distance inland was greater for the larger sizes.

Hama and Takagi (1970) measured the change in total mass and number of giant ASSP with increasing distance inland. They took samples along the bank of the Tedori River, Japan. Their measurements were all taken within one kilometer of the beach. They found that when the wind was onshore at about two m/sec, both number and mass of ASSP fell off rapidly in the first 300 meters from the beach. The concentration at 300 meters from the beach was about five percent of the amount at the beach. Further from the beach the concentrations decreased more slowly, being about two percent at one kilometer. For an onshore wind of 8.5 m/sec they found a similar sharp decrease in the first 300 meters from the beach, the mass and number of giant ASSP dropping to 20% of that at the beach and a concentration of 15% at one kilometer.

The work of Lodge is roughly in agreement with that of Hama and Takagi in the first kilometer from the beach. They seem to agree that the number of giant sea-salt particles at 1/2 km from the beach with a 10 knot wind is about 20% of that at the beach. They agree further that out to one km inland there is a much gentler decrease of sea-salt. Hama and Takagi took no measurements further

inland than one km.

Twomey's work is not directly comparable to Lodge's or Hama and Takagi's because Twomey was sampling from an airplane at altitudes up to 2700 m, while the others were on the ground.

Tanaka (1966) has proposed a theoretical model of the distribution of giant ASSP over land. This model is of particular interest to this study, since the data collected for this study provide an opportunity to try Tanaka's proposed model. The transport and distribution of giant ASSP inland from the coast are studied on the basis of diffusion theory. This model and the fit of the data to it will be discussed in detail in Chapter VI.

III. THE METHOD

The method used to detect and measure the size of ASSP in this study is a microchemical technique which depends upon the halides (Cl^-, Br^-, and Fl^-) in sea-salt particles forming a precipitate when treated with mercurous fluorosilicate. This method was first suggested by Seely (1952) and was refined for field work by Lodge (1954).

ASSP are collected on a membrane filter by drawing air through the filter with a vacuum pump. The filters are 47 mm discs of a paper-like substance. They are manufactured by Millipore Corporation as filter #AAWP04700. Extensive work by Lodge (1954) has shown these filters to be well suited to the collection of ASSP. To obtain a sample the filters are mounted in a holder (also supplied by Millipore) and air is drawn through the filter for 5 to 15 minutes. The flow rate is measured with an air flow meter and is usually 25 liters per minute. The sea-salt particles impinge upon the inlet side of the filter and stick there.

After the filter is exposed it is taken back to the laboratory to be examined. The actual ASSP are not visible under an optical microscope. The salt particles must be enlarged to be visible. To accomplish this the filters are treated with a solution of mercurous fluorosilicate in dilute fluosilisic acid. Each ASSP forms a circular bluish-white halo composed of very fine crystals of mercurous

chloride, bromide, and fluoride. Essentially all of the crystal is mercurous chloride since the ratios $\frac{Cl}{Br}$ and $\frac{Cl}{F}$ in sea-water are 290 and 13, 500 respectively. Lodge and Tufts (1956) have determined that the size of the circular halos on the filters after this treatment is related to the original sea-salt particle dry size. They found the diameter of the reaction halos to be 4.73 times the diameter of the original ASSP. This growth factor applies to all particles with an original dry diameter greater than 1 μ and was used in this study to infer the size of the original ASSP.

Following the treatment with fluorosilicate solution the filters are dried for three hours and then mounted on glass microscope slides. These filters are manufactured such that they become transparent when microscope immersion oil of refractive index 1.515 is applied. The filters are then examined through a Zeiss model TGZ3 microscope using dark field illumination and cross polarized light.

The task of counting and sizing the halos on the filters is time consuming. It is simplified somewhat by counting only the halos found in a few selected microscope fields on the exposed portion of each filter. The microscope fields selected are photographed using a magnification of 125X. From the photomicrographs large prints are made that can be used on the Zeiss model 122 Small Particle Analyzer. These prints are 18 x 27 cm and are made on very thin Kodak projection paper. The Zeiss counter simplifies the task of putting the

reaction halos of the particles into size classes, so that a size distribution can be determined. A disc of light is matched to each halo on the print and the counter automatically registers the halo in the size class to which it belongs.

The Zeiss Analyzer as used separates the particles into 48 equal width diameter intervals. The smallest diameter class (number one on the counter) will contain particles with an original (assumed dry and spherical) diameter of .463 - .850μ. Class number two will include particles with diameters .850 - 1.24μ and so on up to class 48 which contains particles of diameters 17.42 - 17.81μ. The diameter interval of each size class is the same -- .387μ.

ASSP which fell into class one or two on the Zeiss Analyzer were not used in this study because these particles are too small on the prints to be sized accurately. Also background contamination on the filters fell into these size classes and was difficult to distinguish from ASSP halos. Practically all the particles on the prints were smaller than a size class 20 corresponding to a 7.8μ ASSP.

Several prints are analyzed for each filter, the number of prints depending on how many ASSP are in each microscope field. Some filters have a sufficient concentration of ASSP to determine a size distribution with only three prints and some have such a low concentration of particles that ten or more prints are required.

The actual number per liter of ASSP of size class i is given by

$$N_i = \frac{C_i R}{nV}$$

where R is the ratio of the exposed area of a filter to the area of one microscope field (print), n is the number of prints evaluated for that filter, C_i is the number of particles counted in n prints, and V is the volume of air in liters that is drawn through the filter. R is 1820 in this study and V is between 100 and 500 liters. Larger volumes of air are drawn in areas where the expected concentration of ASSP is low so that a sufficient number of particles will be on the prints to determine a size distribution.

IV. THE DATA

A total of 67 samples of ASSP were collected on four separate days. On three of the days samples were taken inland and on one day samples were collected at sea off Oregon. In some cases a sampling site was visited more than once on the same day.

The weather while sampling December 22, 1970 was cool, 40-42°F with 90-100% stratus type cloud cover and 95% average relative humidity. The wind was 2-4 knots and easterly at most stations. There was no rain while samples were being taken. April 16, 1971 had 100% cloud cover, temperature 45-48°F, 90% average relative humidity, wind 3-5 knots southeasterly, and there was intermittent light rain. July 14, 1971 was warm (65-70°F) and sunny with less than 10% average cloud cover. The wind was 5-10 knots from the northwest and the relative humidity averaged 70%. The samples collected at sea were taken over a period of three days and the weather conditions were different for each sample.

Determining the inland profile of ASSP is made difficult by the fact that the concentration at a fixed point may change with time. The supply of ASSP at the coast may vary due to a change in sea state or wind conditions. The rate of fallout of ASSP increases with relative humidity, altering the concentration of ASSP. A change of air mass or a shift in wind direction can cause time fluctuations of ASSP. The

sampling program of July 14, 1971 was designed to obtain a more accurate profile through repeated measurements at the same locations. Six sampling sites along highway 20 between Newport, Oregon and 50 km inland were selected and samples taken at various times during the day at each site. All samples were taken during a period of ten hours. No two samples were collected simultaneously since only one mobile unit (pickup truck) was used to gather all samples. Each station was sampled on a drive towards the coast, then each station was sampled moving away from the coast, and so on for three round trips, producing six horizontal profiles. A time average of the results from each station should then produce an average horizontal profile of ASSP.

The data from the filters consist of the number of ASSP per liter for each of 35 equal width size ranges. Table 4.1 presents the numbers of ASSP in the indicated size classes for the 67 filters used in this study.

Table 4.1. Raw data--number of sea-salt particles per liter per size class. (A blank space for size classes >5 indicates zero.)

Size class	Filter number 1	2	3	4	5	6	7	8	9	10
Distance from beach (km)	33.1	14.2	8.1	.5	4.3	4.6*	138.9*	28*	14.2	11.4
Wind speed (kts)	3	3	1	3	2	15	20	4	4	2
Relative humidity (%)	97	92	96	96	95	84	82	84	97	85
3	42.8	29.3	20.6	161.5	183.7	588.9	449.5	115.1		
4	19.8	13.5	13.5	150.4	112.4	416.1	245.5	59.7	81.5	71.9
5	11.1	5.5	10.3	83.9	80.8	128.0	113.3	33.8	33.2	27.6
6	1.6	3.2	8.7	61.8	39.6	96.0	60.4	17.1	13.8	9.7
7	.8	2.4	.8	33.3	33.3	64.0	11.3	10.4	6.9	1.4
8	2.4	2.4	.8	33.3	7.9	25.6	11.3	7.0	1.4	1.4
9	1.6		.8	22.2	17.4	25.6	15.1	1.8		
10			.8	19.0	6.3	6.4		1.6	1.4	
11	.8			3.2	6.3	6.4		1.1	1.4	
12			.8	7.9	1.6	6.4	3.9	.4		
13			.8	9.5	4.8	6.4				
14				4.8	1.6			.5		
15				6.3	3.2					
16				7.9				.2		
17				4.8	1.6			.2		
18				3.2						
19				4.8						
20				1.6				.2		
21										
22				1.6						
23										
24										
>24					3.2					

* Indicates samples taken at sea.

Table 4.1. (continued)

Size class	Filter number									
	11	12	13	14	15	16	17	18	19	20
Distance from beach (dm)	.3	4.3	6.5	10.2	14.2	.3	2.4	4.3	10.2	14.2
Wind speed (kts)	6	4	4	0	4	15	12	7	5	4
Relative humidity (%)	90	78	90	79	95	90	95	90	87	95
3										
4	102.3	91.6	59.5	41.5	26.7	635.8	160.3	245.3	176.2	190.0
5	33.2	31.1	16.1	19.4	8.3	331.7	78.8	138.2	89.8	90.2
6	13.8	6.9	4.6	8.3	1.8	193.5	38.7	57.0	43.8	44.2
7	8.3	5.2	4.6	4.2	.9	96.8	26.3	29.4	20.7	19.2
8	5.5	1.7	2.3	1.4	.9	62.2	9.7	15.6	16.1	7.7
9		1.7		2.8		41.5	4.2	5.2	13.8	5.8
10	5.5			1.4	.9	20.7	1.4	10.4	4.6	7.7
11	2.8					31.1	1.4	6.9	2.3	3.8
12						13.8		3.5	3.5	1.9
13						17.3		3.5	1.2	1.9
14								1.7		1.9
15						13.8	1.4	1.7	2.3	
16							1.4		1.2	1.9
17						3.5	1.4			1.9
18						3.5				
19										
20									2.3	
21						6.9			1.2	
22								1.5	2.3	
23										
24								1.5	2.3	
> 24										

Table 4.1. (continued)

Size class	Filter number									
	21	22	23	24	25	26	27	28	29	30
Distance from beach (km)	1.9*	9.3*	18.5*	27.8*	83.3*	120.2*	120.2*	120.2*	120.2*	157.3*
Wind speed (kts)	18	20	18	15	6	2	2	3	3	12
Relative humidity (%)	100	87	88	76	85	73	73	73	73	85
3	348.8	603.8	541.1	527.7	192.3	102.9	98.4	147.6	107.3	142.2
4	184.5	487.4	456.1	322.0	129.7	85.0	82.7	109.6	75.5	69.8
5	70.4	192.3	210.2	138.6	80.5	42.5	47.0	47.0	41.9	45.6
6	50.3	102.9	76.0	62.6	29.1	47.0	22.4	29.1	23.5	16.1
7	20.1	58.1	44.7	44.7	20.1	24.6	20.1	24.6	18.4	10.7
8	6.7	4.5	40.2	26.8	40.2	17.9	13.4	8.9	8.4	8.1
9	6.7	26.8	17.9	35.8	11.2	4.5	4.5	6.7	8.4	
10		17.9		4.5	17.9	4.5	2.2	11.2	3.4	5.4
11		8.9	17.9	4.5		2.2	2.2	4.5	5.0	
12		13.4	13.4	8.9		2.2	2.2	6.7	1.7	
13		4.5			2.2	4.5				
14		8.9	4.5			2.2	2.2		3.4	
15					2.2					
16										
17										
18			4.5	4.5						
19										
20										
21										
22										
23										
24										
> 24										

* Indicates samples taken at sea.

Table 4.1. (continued)

Size class	Filter number									
	31	32	33	34	35	36	37	38	39	40
Distance from beach (km)	194.5*	27.8*	18.5*	9.3*	1.9*	50.7	33.1	14.2	11.4	4.3
Wind speed (kts)	12	15	20	20	23	1	4	3	3	2
Relative humidity (%)	94	77	79	82	82	74	81	73	72	67
3	72.4	322.0	231.4	298.5	264.9	13.4	17.9	38.6	131.9	206.8
4	26.8	171.0	147.6	154.3	171.0	2.2	3.6	9.2	74.9	111.8
5	18.8	87.2	80.5	90.6	134.2	2.9	1.8	2.5	34.7	49.2
6	10.7	47.0	47.0	53.7	67.1			.8	16.8	29.1
7	8.1	20.1	20.1	13.4	16.8	2.2			10.1	19.0
8	5.4	26.8	3.4	30.2	36.9			.8	12.3	10.1
9		10.1	6.7	16.9	23.5				10.1	5.6
10			6.7		13.4				1.1	3.4
11		3.4		3.4	3.4				3.4	1.1
12			3.4	3.4	10.1				1.1	2.2
13										2.2
14		3.4		3.4	3.4				2.2	3.4
15	2.7	3.4							1.1	
16										
17		3.4								
18		3.4								
19										1.1
20										1.1
21										
22		3.4								
23										
24										
> 24										

* Indicates samples taken at sea.

Table 4.1. (continued)

Size class	Filter number									
	41	42	43	44	45	46	47	48	49	50
Distance from beach (km)	.3	2.4	4.3	10.2	14.2	33.1	14.2	10.2	4.3	2.4
Wind speed (kts)	15	5	7	4	4	5	4	3	4	5
Relative humidity (%)	90	74	63	62	62	57	64	65	67	72
3	479.6	550.0	241.7	125.2	131.5	36.5	213.0	236.4	372.1	689.5
4	348.8	297.4	132.8	86.1	76.5	14.9	112.4	134.1	172.8	273.7
5	157.6	109.6	56.0	32.4	41.6	8.2	46.9	58.7	86.4	131.5
6	134.2	60.4	19.2	19.0	26.8	3.7	36.9	45.3	36.0	75.1
7	80.5	22.4	16.0	7.8	9.4	5.2	13.4	18.4	14.4	51.0
8	57.0	13.4	6.4	5.6	5.4	1.5	3.4	6.7	12.0	24.0
9	36.9	6.7		4.5	10.7		5.0	3.4	9.6	13.4
10	30.2	2.2	3.2	2.2	5.4	1.5	3.4	5.0	2.4	13.4
11	23.5	8.9		1.1		1.5		3.4	4.8	2.7
12	13.4	2.2	1.6	1.1			1.7	1.7		8.1
13	3.4	2.2								10.7
14	10.1				1.3	1.5	1.7			2.7
15		2.2								2.7
16										
17	13.4							1.7	4.8	
18	6.7									
19		2.2								
20										
21	3.4									
22										
23	3.4									
24										
>24	6.8								2.4	2.7

Table 4.1. (continued)

Size class	Filter number									
	51	52	53	54	55	56	57	58	59	60
Distance from beach (km)	.3	2.4	6.5	10.2	14.2	33.1	14.2	10.2	4.3	2.4
Wind speed (kts)	18	5	4	3	4	9	6	7	2	6
Relative humidity (%)	83	74	66	64	65	58	71	66	66	74
3	965.9	965.9	297.7	285.1	291.8	277.2	303.0	270.5	389.0	449.0
4	610.4	493.7	199.7	145.9	152.6	155.0	137.5	158.4	144.2	311.9
5	268.3	198.5	61.5	80.5	85.5	77.5	67.1	73.6	50.3	107.3
6	161.0	99.3	46.1	37.0	36.9	25.3	29.1	22.4	36.9	57.01
7	114.0	42.9	30.7	16.8	16.8	26.8	16.8	16.0	43.6	30.2
8	80.5	40.2	9.6	8.4	8.4	10.4	3.4	4.8	20.1	26.8
9	33.5		13.4	5.0	10.1	3.0	5.6	1.6	6.7	6.7
10	20.1	5.4	5.8		3.4	1.5	2.2	4.8	3.4	6.7
11	26.8	8.1		1.7	3.4	1.5	3.4			3.4
12	13.4	8.1	1.9					3.4		
13	6.7	2.7								
14	6.7		1.9							3.4
15	13.4				3.4			1.6	3.4	
16										
17		2.7								
18	20.1									
19	6.7		1.9							
20										
21	13.4									3.35
22										
23	13.4									
24	6.7									
>24	6.7									

Table 4.1. (continued)

Size class	Filter number						
	61	62	63	64	65	66	67
Distance from beach (km)	.3	2.4	6.5	10.2	14.2	33.1	50.7
Wind speed (kts)	15	15	3	4	4	5	3
Relative humidity (%)	88	74	71	70	76	70	66
3	956.9	399.1	362.2	342.1	278.4	232.6	150.2
4	728.8	315.3	174.4	160.9	202.9	176.1	93.0
5	380.1	150.9	67.1	89.4	109.0	109.1	41.1
6	272.8	97.3	67.1	44.7	52.0	70.4	16.1
7	201.2	36.9	20.1	24.6	25.2	20.1	4.5
8	107.3	33.5	23.5	13.4	20.1	11.7	4.5
9	93.9	13.4	13.4	6.7	10.1	10.1	1.8
10	31.3	6.7	6.7	8.9	6.7	5.0	
11	35.8	3.4	6.7		1.7		.9
12	31.3	3.4	3.4	2.24	5.0	1.7	
13	8.9	3.4			1.7		.9
14	13.4		3.4				
15	13.4		10.1		1.7		
16							
17	8.9					1.7	
18	4.5	3.4			3.4		
19					1.6		
20							
21							
22	4.5						
23	4.5	3.4	3.4				
24							
> 24	9.0						

V. ANALYSIS OF DATA

The data were initially examined by plotting the frequency of occurence of particles in a size class against particle dry diameter. The resulting histograms had two features that were common to all the samples in this study. Each size class had more particles than the next size class larger, with exceptions that could have been statistical fluctuations. The data from each filter appeared to follow an exponential diameter distribution with a different parameter of the exponential for each filter. Figure 5.1 is an example of two of these histograms.

Problems with the Raw Data

One problem with the size distributions obtained from the Zeiss analyzer is that the diameter distribution is discrete, that is each individual particle belongs to a size range. We would like to have the more realistic smooth relative frequency distribution.

Another problem with the discrete size distributions is the erratic data in the tail of the distribution for the relatively large particles. For example in Figure 5.1(b) size class seven has 12 particles per liter and yet size class nine has 16 particles per liter. This type of fluctuation is probably due to too few actual particles of these sizes being counted. The accuracy of a determination of particle concentration depends on the number of particles

that are counted. Hence the concentrations for the smaller particles are relatively more accurate than the concentrations for the larger particles.

It was also evident that some of the distribution data for the smaller particle sizes sometimes exhibited fluctuations which were due either to sampling or counting errors. Notice, for example that size class five, Figure 5.2 is much lower than it should be to fit in with the general trend of the other classes.

Fitting a Smooth Curve to the Data

Because of these problems with the discrete distribution data it was decided to try to fit a smooth curve through the data. A curve was desired that would smooth out the fluctuations, give information on the size distribution within a size class, and possibly permit some extrapolation of the size distribution into sizes that were not actually counted. It was found that when the natural logarithm of the number of particles was plotted against particle diameter for a particular filter, the data fell approximately along a straight line with random fluctuations about the line. This suggested an exponential distribution of number of particles versus particle diameter.

After examining graphically the size distribution of about one-half of the filters, it was decided to find the exponential density function for each sample which best fit the observed frequencies.

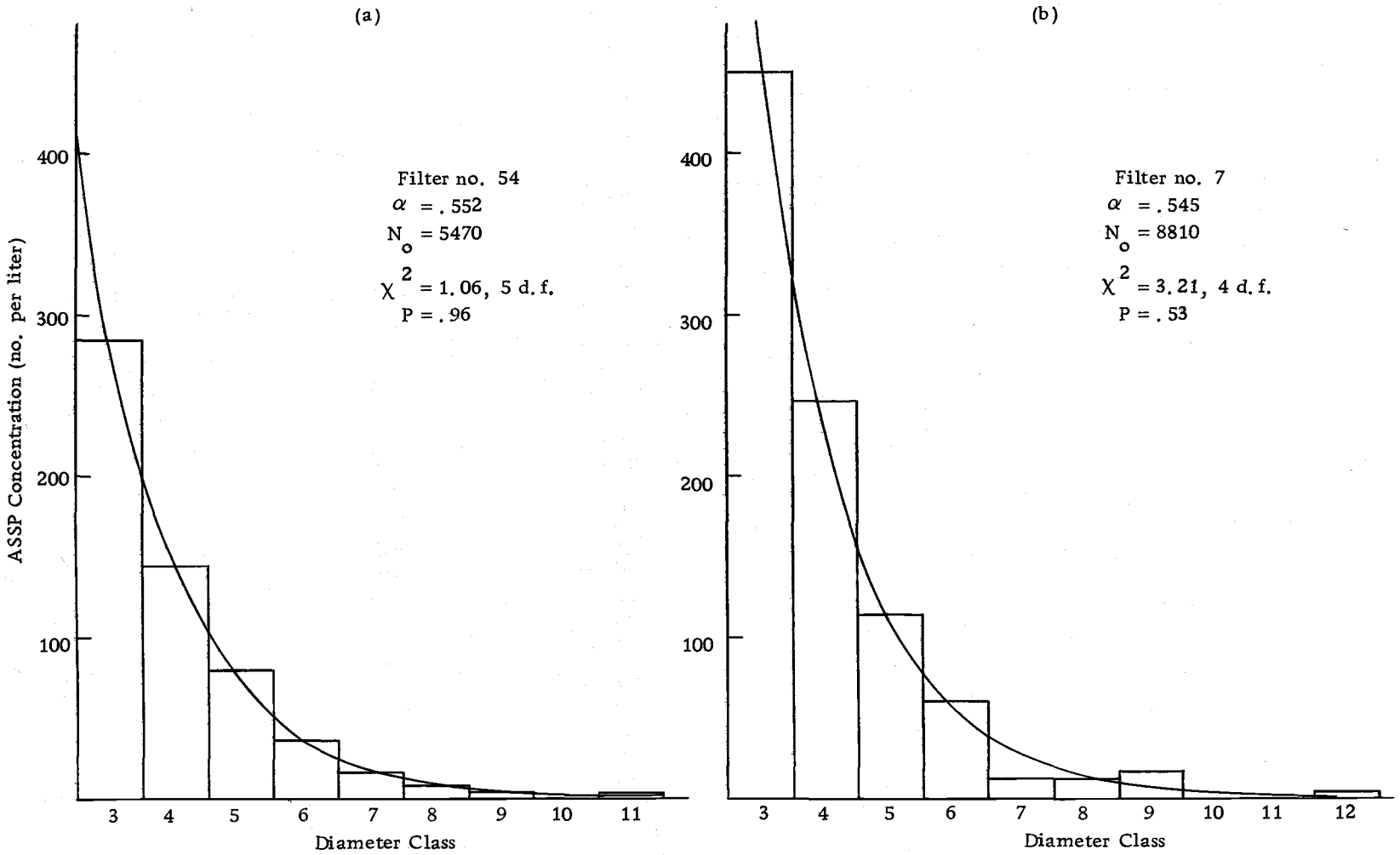

Figure 5.1. Two examples of the data fitted with an exponential curve.

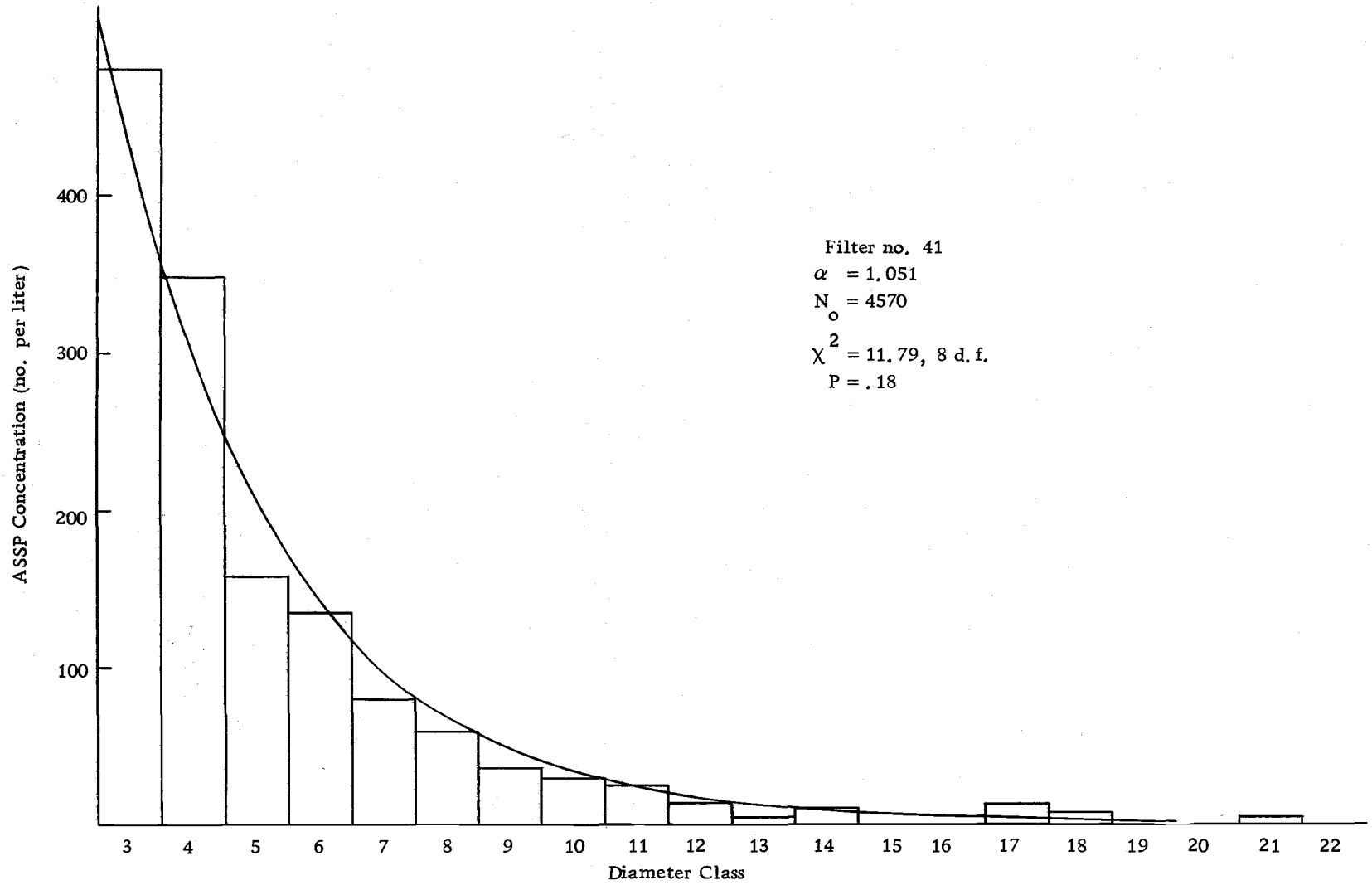

Figure 5.2. Data from filter no. 41 fitted with an exponential curve

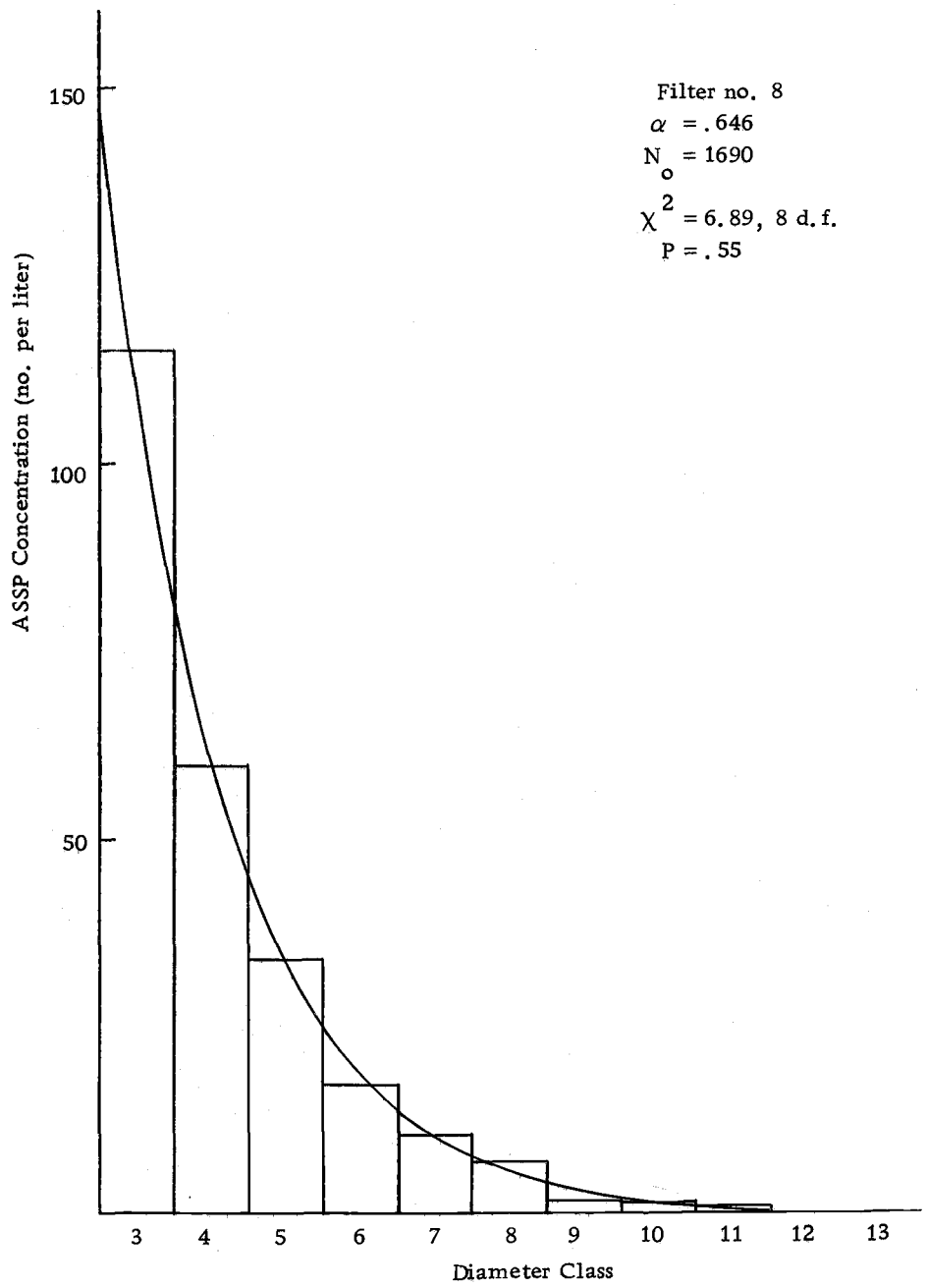

Figure 5.3. Data from filter no. 8 fitted with an exponential curve.

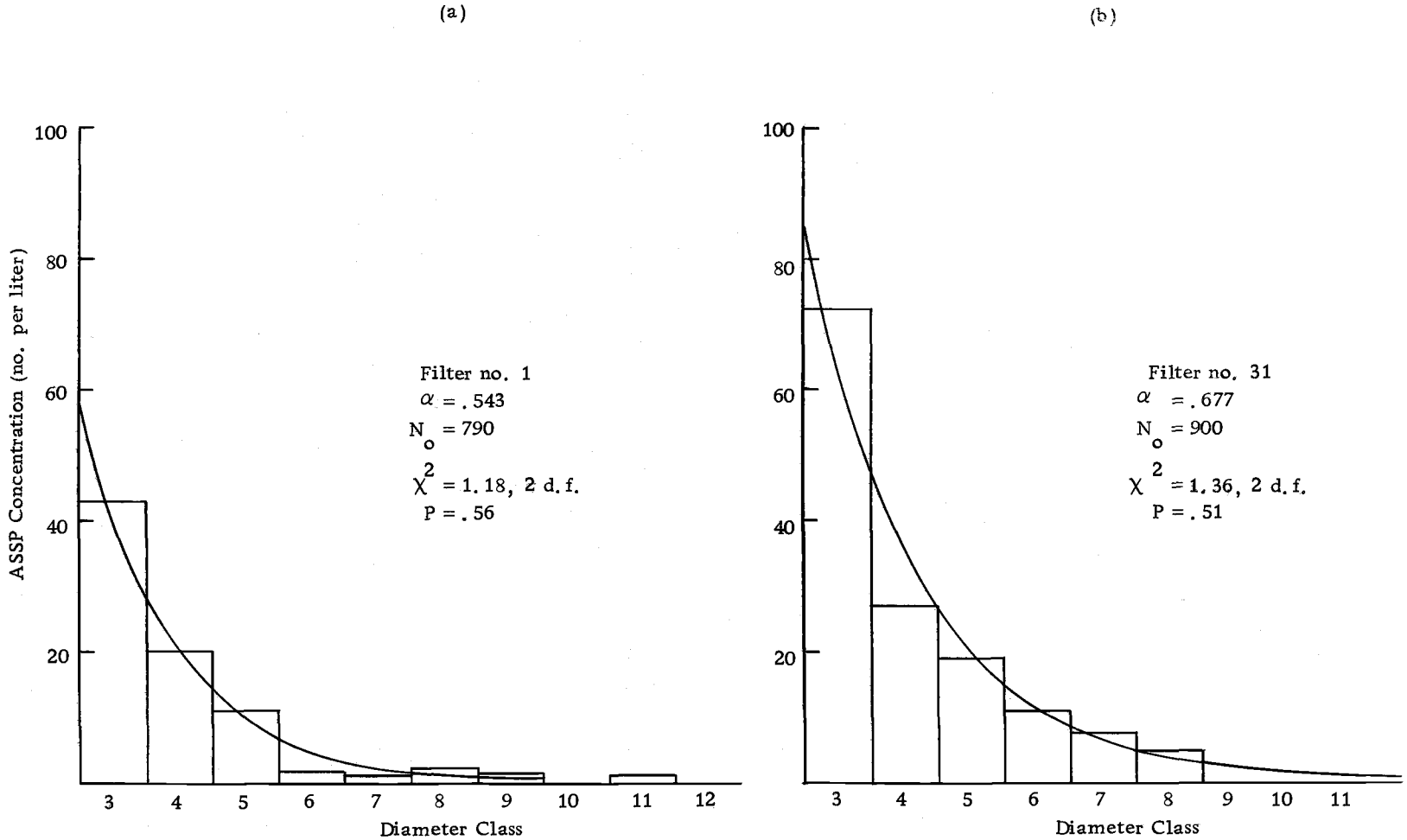

Figure 5.4. Two examples of the data fitted with an exponential curve.

The exponential random variable has distribution function

$$F(x) = 0 \qquad x < 0$$
$$= 1 - e^{-x/\alpha} \qquad x \geq 0$$

and probability density function

$$f(x) = \frac{1}{\alpha} e^{-x/\alpha} \qquad x > 0$$
$$= 0 \quad \text{otherwise.}$$

Since the probability density function gives relative frequencies, it was necessary to multiply it by a constant, N_0, to get actual number frequencies. The number frequency is then:

$$N(x) = N_0 f(x) = \frac{N_0}{\alpha} e^{-x/\alpha} \quad x > 0 .$$

α is the parameter which determines the steepness or relative rate of decrease of the exponential curve. A larger α will give a more gradual exponential decrease. α also turns out to be the average or expected particle diameter:

$$E(x) = \int_0^\infty x \frac{x}{\alpha} e^{-x/\alpha} dx = \alpha .$$

This property of α is probably not significant here because α is always smaller than the smallest particle counted. N_0 determines the level of concentration for a given value of α N_0 is also the total number of particles of all sizes for this distribution:

$$N_{total} = \int_0^\infty \frac{N_0}{\alpha} e^{-x/\alpha} dx = N_0 .$$

The maximum likelihood estimator[1/] for N_0 and α was used

[1/] For a discussion of maximum likelihood estimators see for example Hogg and Craig (1968) p. 243.

to fit an exponential density function to each set of data. Maximum likelihood gives an estimate for α and N_0 based on the jointly sufficient statistics for these parameters. Appendix A gives the details of how N_0 and α were found by this method. The results of using the maximum likelihood method in this case are:

$$\alpha = \frac{h}{\ln(1 + \frac{N}{S})} \quad \text{where} \quad S = \sum_{i=1}^{k} (i-1)M_i$$

M_i = the individual class frequencies

$N = M_1 + M_2 + \cdots M_k$

h = diameter interval (.3872μ)

$$N_0 = N(1 + \frac{N}{S})^{x_1/h}$$

x_1 = lower boundary of diameter class one

A computer program was written that would compute α and N_0 from the M_i and diameter intervals for each sample. The program also gave the χ^2 goodness-of-fit statistic for each set of data. This statistic is

$$\chi^2 = \sum_{i=1}^{k} \frac{(M_i - N_0 p_i)^2}{N_0 p_i}$$

where M_i is the observed frequency in class i and $N_0 p_i$ is the expected frequency computed from the fitted exponential curve. Only size classes with an expected frequency of at least five particles were used in computing the sample χ^2. All classes which had an expected frequency of less than five particles were combined to make one size class. Table 5.1 presents the fitted values of α and N_0 and the sample χ^2 and number of degrees of freedom for

Table 5.1. Fitted values of the parameters of the size distribution.

Filter no.	Km From Beach	$\hat{\alpha}$	$\hat{N}_o$	M_{tot}^x 10^9 gm/l	χ^2	Degrees of Freedom	$P(>\chi^2)$
1	33.1	.5426	790	.83	1.18	2	.56
2	14.2	.5531	527	.59	.68	2	.73
3	8.1	.7981	272	.91	5.61	3	.23
4	.5	1.2681	1647	22.16	19.08	9	.024
5	4.3	.9386	1882	10.26	8.68	7	.28
6	4.6*	.6596	8939	16.92	6.75	5	.24
7	138.9*	.5452	8806	9.41	3.21	4	.53
8	28.0*	.6457	1693	3.01	6.89	8	.55
9	14.2	.4579	4849	3.07	.09	2	.96
10	11.4	.3550	10874	3.21	.77	2	.69
11	.3	.5325	3622	3.61	2.51	2	.30
12	4.3	.3737	10672	3.68	1.57	2	.44
13	6.5	.3748	6676	2.32	.44	1	.50
14	10.2	.5543	1558	1.66	.19	2	.91
15	14.2	.3965	2383	.98	.50	1	.49
16	.3	.8191	10694	38.78	17.83	7	.014
17	2.4	.6046	4769	6.95	1.52	4	.82
18	4.3	.6889	5510	11.88	13.35	5	.021
19	10.2	.8223	2765	10.14	17.68	6	.008
20	14.2	.6542	4530	8.37	7.21	4	.14
21	1.9*	.5251	7254	6.93	2.06	4	.73
22	9.3*	.6965	9036	20.14	21.13	6	.002
23	18.5*	.7113	8121	19.28	14.67	6	.024
24	27.8*	.6768	7346	15.02	6.50	5	.26
25	83.3*	.8428	2281	9.01	15.43	6	.019
26	120.2*	.9368	1273	7.87	5.44	5	.38
27	120.2*	.8248	1333	4.93	2.55	4	.64
28	120.2*	.8125	1814	6.42	5.57	5	.37
29	120.2*	.8459	1281	5.12	1.43	5	.91
30	157.3*	.6020	2325	3.39	.90	3	.82
31	194.5*	.6771	901	1.84	1.36	2	.51
32	27.8*	.7408	3742	10.04	5.09	5	.42
33	18.5*	.6446	3726	6.58	1.65	4	.80
34	9.3*	.6951	3957	8.77	6.09	5	.31
35	1.9*	.8450	3219	12.81	8.24	6	.23
36	50.7	.4862	266	.20	2.98	1	.09
37	33.1	.2676	2369	.30	.003	0	
38	14.2	.3105	2796	.55	.08	1	.79
39	10.2	.7446	1578	4.30	9.87	5	.08
40	4.3	.7018	2600	5.93	8.57	6	.21
41	.3	1.0510	4571	35.01	11.79	8	.18
42	2.4	.5611	9796	11.41	8.53	5	.14
43	4.3	.5233	5072	4.80	3.08	4	.55
44	10.2	.6199	2097	3.30	5.51	5	.37
45	14.2	.7045	1787	4.12	4.68	5	.46
46	33.1	.7079	424	.99	5.39	3	.16

Table 5.1. (continued)

Filter no.	Km From Beach	$\hat{\alpha}$	$\hat{N}_o$	$M_{tot} \times 10^9$ gm/l	χ^2	Degrees of Freedom	$P(>\chi^2)$
47	14.2	.5924	3523	4.85	2.42	4	.66
48	10.2	.6369	3591	6.12	3.43	5	.64
49	4.3	.6069	5512	8.13	7.62	5	.19
50	2.4	.6461	8829	15.71	26.57	6	.001
51	.3	.9383	8926	48.65	23.37	7	.002
52	2.4	.5441	18147	19.28	6.17	5	.30
53	6.5	.6493	4506	8.14	11.25	5	.047
54	10.2	.5516	5467	6.05	1.06	5	.96
55	14.2	.6298	4376	7.21	4.95	5	.43
56	33.1	.5637	5191	6.14	6.80	5	.24
57	14.2	.5236	6033	5.71	5.19	5	.41
58	10.2	.5364	5502	5.60	4.94	4	.31
59	4.3	.5951	5605	7.79	16.85	4	.002
60	2.4	.6214	7367	11.66	8.34	5	.15
61	.3	.9784	10293	63.60	9.23	9	.43
62	2.4	.7412	5679	15.25	7.10	6	.32
63	6.5	.7588	3888	11.20	12.26	5	.033
64	10.2	.5987	5473	7.75	1.06	5	.96
65	14.2	.7464	3774	10.35	7.27	6	.31
66	33.1	.6406	5032	8.73	6.64	6	.37
67	50.7	.5297	3235	3.17	7.11	4	.14

*Indicates samples taken at sea.

the samples used in this study. The number of degrees of freedom is the number of classes from which χ^2 is calculated less two--one extra degree of freedom is removed for the estimation of α. Figures 5.1-5.4 are examples of the raw data and the fitted curves.

The question arises as to whether the fitted family of exponential distribution functions is an accurate description of the ASSP diameter distribution data. In addition to random fluctuations about the fitted distribution there may be systematic errors due to deviation of the observed distribution from the assumed form. It is difficult to judge from direct inspection of the data and fitted curves whether the deviations from the fitted curves are random or systematic.

This question was therefore investigated statistically using the values of the χ^2 goodness-of-fit statistic that were computed for each filter. From the sample value of χ^2 and the number of degrees of freedom the probability P, of getting a value of χ^2 equal to or larger than the observed value was determined for each filter. We would expect 10% of these values of P to be .10 or smaller, even if the distribution is of the assumed form. If the proportion of P's with value .10 or smaller is significantly greater than 10%, then the diameter distribution probably is not of the assumed form. It was noticed that the samples taken inland within eight kilometers of the shoreline tended to have low values of P

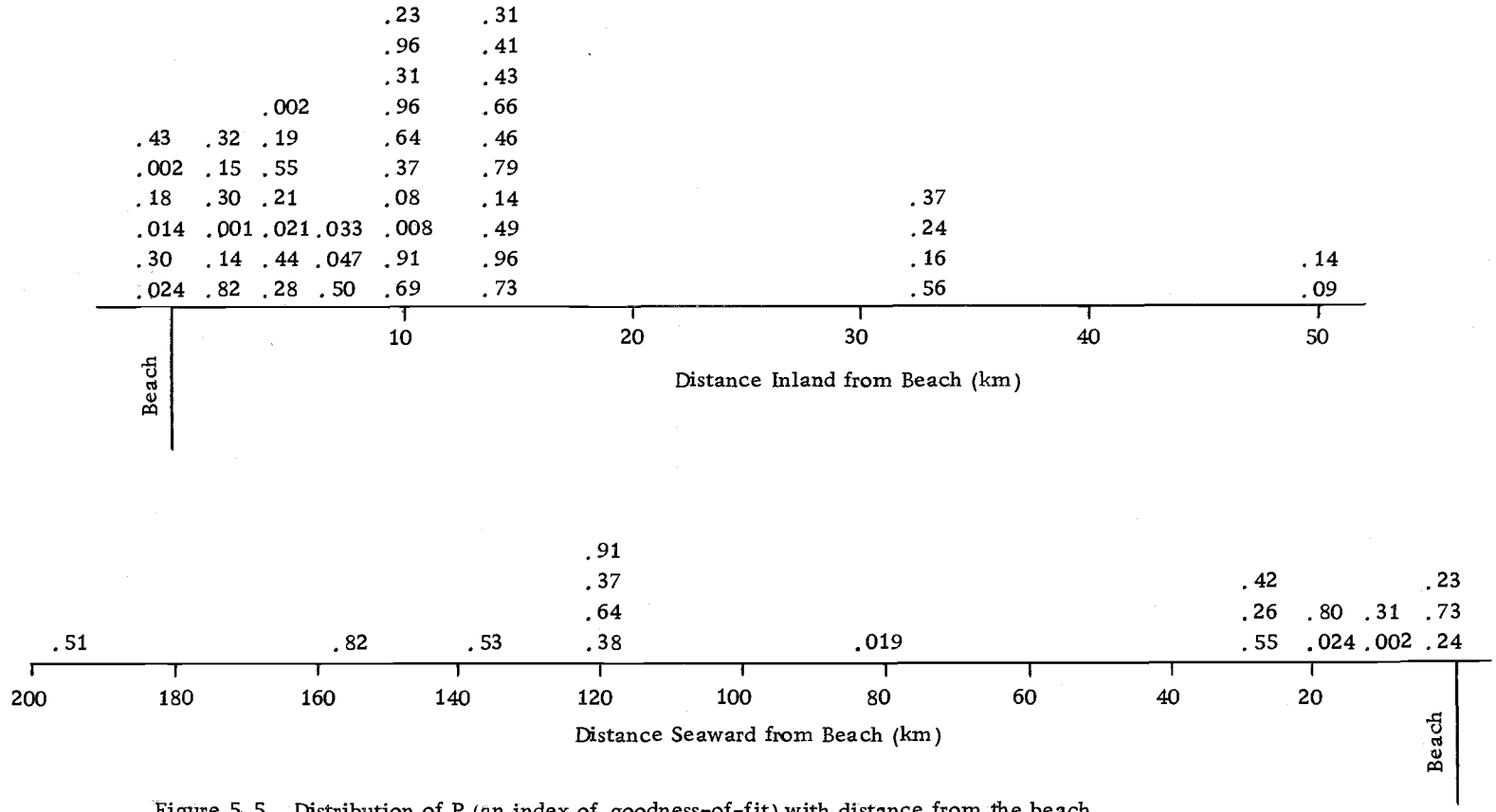

Figure 5.5. Distribution of P (an index of goodness-of-fit) with distance from the beach.

and a relatively large number of P's with value less than .10. The samples taken at sea and greater than eight kilometers inland did not have many values of P less than .10. Figure 5.5 shows the locations where the 66 values of P occurred relative to the shoreline.

It was desired to statistically test whether P was related to distance from the beach and also whether P was related to wind speed or relative humidity. To do this the values of P were classified according to:

	1	2	3
Wind Speed (kts)	$0 - 3\frac{1}{2}$	$3\frac{1}{2} - 8$	$8 - 24$
Relative Humidity (%)	$55 - 72\frac{1}{2}$	$72\frac{1}{2} - 84\frac{1}{2}$	$84\frac{1}{2} - 100$
Distance from Beach (km)	at sea	0-8 km inland	>8 km inland

Using this three-way classification an analysis of variance was done to test the null hypotheses:

Ho_1 The mean values of P for the three classifications of wind speed are not significantly different.

Ho_2 The mean values of P for the three classifications of relative humidity are not significantly different.

Ho_3 The mean values of P for the three classifications of distance are not significantly different.

Table 5.2 presents the results of this analysis of variance and the

Table 5.2. Results of analysis of variance and F-tests on P.

Source of Variation	Degrees of Freedom	Sum of Squares
Wind Speed	61	4.4513
Relative Humidity	61	4.5112
Distance from Beach	61	5.1562
Determinations (Error)	59	4.4224

To test Ho_1:

$$\text{Test criterion} = F_{WS} = \frac{(SS_{WS} - SS_E)/(61-59)}{SS_E/59} = .1927$$

$$F^{2}_{59}(2.5\% \text{ level}) = 3.93 \rightarrow Ho_1 \text{ not rejected}$$

To test Ho_2:

$$\text{Test criterion} = F_{RH} = \frac{(SS_{RH} - SS_E)/(61-59)}{SS_E/59} = .5925$$

$$F^{2}_{59}(2.5\% \text{ level}) = 3.93 \rightarrow Ho_2 \text{ not rejected}$$

To test Ho_3:

$$\text{Test criterion} = F_{D} = \frac{(SS_{D} - SS_E)/(61-59)}{SS_E/59} = 4.8947$$

$$F^{2}_{59}(2.5\% \text{ level}) = 3.93 \rightarrow Ho_3 \text{ rejected}$$

samples values of F that were obtained.[2/]

The F-tests on wind speed and relative humidity indicate non-significance, hence we cannot reject the null hypotheses concerning them. The conclusion is that P, an index of goodness-of-fit of the size distribution, does not vary significantly with either wind speed or relative humidity for this data. The F value for the distance classification is strongly significant, indicating rejection of the null hypothesis concerning distance from the beach even at the 2.5% significance level. The probability of a Type I error (rejection of the null hypothesis when it is true) is only about .02.

Having established that there are significant differences among the mean values of P for the distance classifications, the distance class means were examined to see where the differences occurred and to determine which differences were significant. The Least Significant Difference (LSD) method was used in comparing means. The difference between a specific pair of means is significant at the 5% level if it exceeds the quantity $\sqrt{s^2(\frac{1}{n_i} + \frac{1}{n_k})}\, t_{.05}$, caled the Least Significant Difference. $\sqrt{s^2(\frac{1}{n_i} + \frac{1}{n_k})}$ is the standard error of the difference between two means, with degrees of freedom equal to those in s(63). n_i is the number of observations in the mean, $\overline{P_i}$, for distance class i. The differences that

---

[2/] In the analysis of variance the F-test, a test based on the ratio of two variances, is used to test hypotheses concerning population means. (See for example Hogg and Craig (1968), Chapter 12).

were tested and the LSD for each are given in Table 5. 3.

Table 5. 3. Differences among the mean values of P for the three distance classifications.

Difference	Explanation	LSD
$\overline{P}_1 - \overline{P}_2 = .2051$	difference between mean value of P at sea and < 8km inland.	.1648
$\overline{P}_3 - \overline{P}_2 = .2401$	difference between mean value of P >8km inland and < 8km inland	.1557
$\overline{P}_3 - \overline{P}_1 = .0350$	difference between mean value of P at sea and >8km inland	.1708

It can be seen from Table 5. 3 that the mean value of the P's obtained at sea ($\overline{P}_1$) and the mean value of P's from data taken greater than eight kilometers inland ($\overline{P}_3$) are not significantly different because their difference does not exceed the Least Significant Difference for that comparison. The mean, $\overline{P}2$, for the data collected inland within eight kilometers of the shoreline is significantly different from both the other means $\overline{P}_1$ and $\overline{P}_3$ at the 5% significance level. This result supports the conclusion that the ASSP size distribution for samples collected at sea and greater than eight kilometers inland is better fitted by an exponential random variable than is the data collected inland within eight kilometers of the shoreline.

The null hypothesis that the proportion of P's with value .10 or less is not greater than 10% will be rejected for the data from less than eight kilometers inland, but not rejected for either the data at sea or the data from greater than eight kilometers inland. The conclusion is that ASSP diameter distributions observed at sea and greater than eight kilometers inland are well-described by a family of exponential random variables, while data from less than eight kilometers inland are not.

The data from the area less than eight kilometers inland was examined to see how the distribution deviated from exponential. Figure 5.6 shows two examples of the poorly fitted data from less than eight kilometers inland. The general tendency observed in these two cases and the other 20 filters from less than eight kilometers inland is for the fitted exponential distribution to be too low for the lowest size class and too low for the tail of the distribution. The size classes in between are usually overestimated. For example, 19 of the 22 filters from the region less than eight kilometers inland have an estimate of size class five that is too high; 20 of the 22 have an estimate of size class six that is too high.

The filters from near the beach have size distributions that have too many particles in the tail (i.e. the larger particles) to be well-described by an exponential. This is quite likely due to the high production of ASSP of the larger sizes by the action of the surf.

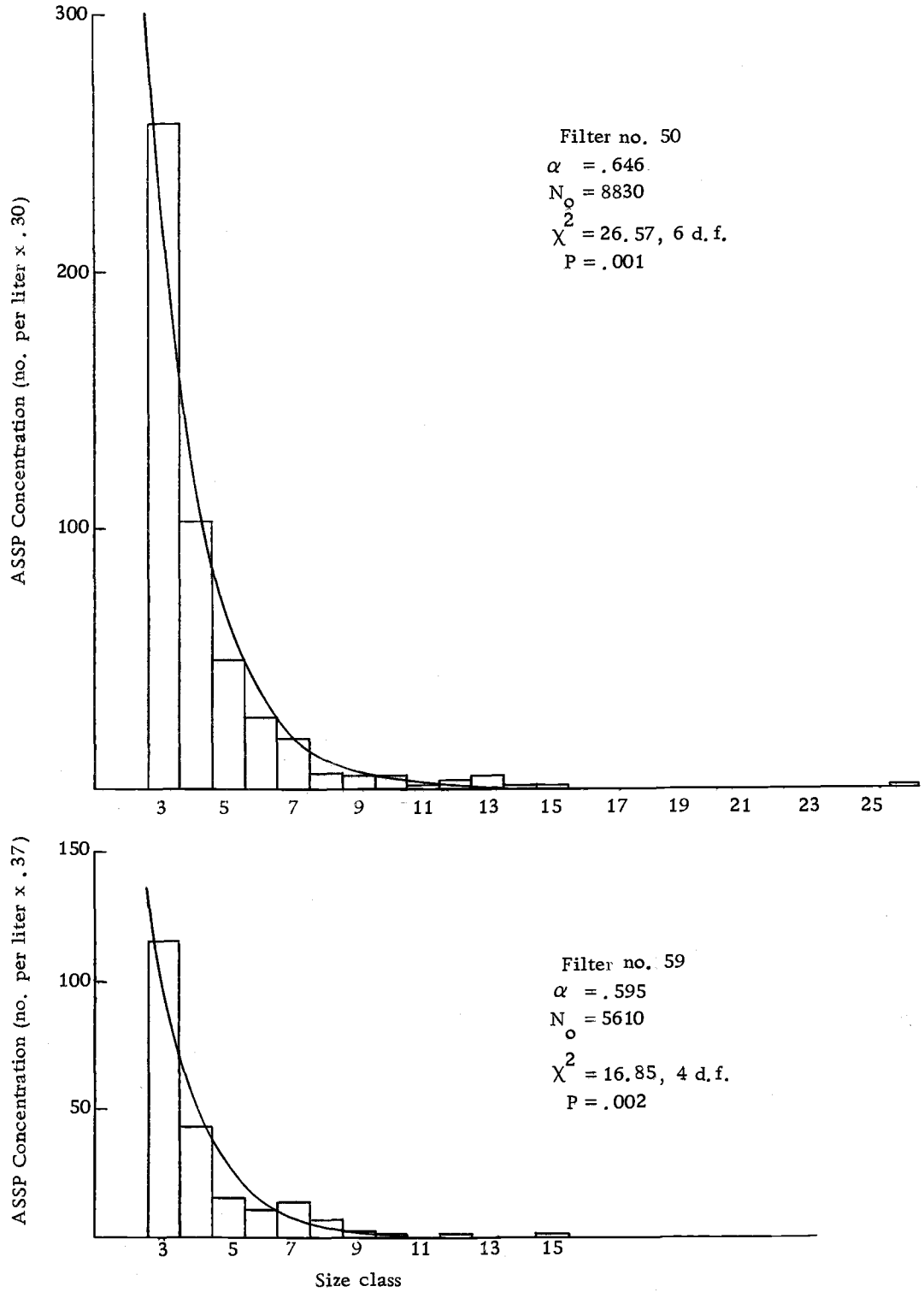

Figure 5.6. Two examples of the poorly fitted size distribution data.

Breaking swell creates a large amount of white water and air bubbles that are efficient producers of ASSP. Evidently the surf contributes a size distribution other than exponential, but as the population of ASSP in an air mass ages or moves inland, an exponential diameter distribution prevails.

An attempt was made to fit a power law of the form $N(x) \propto x^{-\beta}$ to the data from less than eight kilometers inland. For the seven cases that were fitted and χ^2 calculated only three had a P value greater than .10. An examination of the predicted and observed class frequencies revealed why the power law did not fit well. The estimates of the lowest size class, class three, were too high in all seven cases and the estimates of the tail were too high in every case. However, the estimates of the mid-range size classes, from class four to class eight, were predominantly underestimates. It was decided to use only the raw data for the samples taken within eight kilometers of the beach and to use the fitted exponential curves for data from out at sea and greater than eight kilometers inland. Table 5.4 presents the raw data for the samples taken inland within eight kilometers of the beach.

Table 5.4. Observed parameters on mass and number for data from < 8 km inland.

Filter No.	km from Beach	N(d>1.24)	N(d>2.01)	N(d>2.79)	N(d>3.95)	Mass g/l x 10^9 (d>1.24)
4	.5	621.8	308.8	163.1	74.4	25.35
5	4.3	503.6	207.5	87.1	28.5	15.63
11	.3		69.1	22.1	8.3	2.69
12	4.3		46.7	8.6		1.53
13	6.5		27.6	6.9		.97
16	.3		836.2	311.0	110.6	42.02
17	2.4		164.5	47.0	6.9	5.99
18	4.3		273.0	77.7	27.6	13.16
40	4.3	446.0	127.4	49.2	14.5	7.17
41	.3	1408.6	580.2	288.4	114.0	54.81
42	2.4	1079.9	232.5	62.6	20.1	11.96
43	4.3	476.9	102.4	27.2	4.8	4.17
49	4.3	717.8	172.8	50.4	14.4	10.87
50	2.4	1301.2	338.0	131.5	42.9	20.10
51	.3	2387.8	811.6	382.3	154.3	83.60
52	2.4	1867.3	407.8	110.0	26.8	18.49
53	6.5	670.2	172.8	65.3	11.5	8.54
59	4.3	700.9	167.7	80.5	10.1	8.06
60	2.4	1006.1	244.8	80.5	16.8	12.81
61	.3	2906.5	1220.8	567.9	165.5	81.49
62	2.4	1069.8	355.5	107.3	23.5	17.42
63	6.5	761.3	224.7	90.6	33.6	15.29

Uses of the Fitted Exponential Curves

From the fitted exponential size distribution curves several parameters of interest can be easily calculated. The number of giant ASSP ($d > 2\mu$) is:

$$N_2 = \int_2^{\infty} \frac{N_0}{\alpha} e^{-x/\alpha} dx = N_0 e^{-2/\alpha}$$

The number of ASSP in the size class x_i to x_{i+1} is:

$$\int_{x_i}^{x_{i+1}} \frac{N_0}{\alpha} e^{x/\alpha} dx = N_0 \left[e^{-x_i/\alpha} - e^{-x_{i+1}/\alpha} \right] .$$

The number of ASSP in the size range that was actually counted is:

$$N_c = \int_{1.24}^{\infty} \frac{N_0}{\alpha} e^{-x/\alpha} dx = N_0 e^{-1.24/\alpha} .$$

N_c, the concentration found by integrating over the size range actually counted, will always be exactly the same concentration determined from the raw data. This is because in the maximum likelihood method, N_0 was estimated by:

$$N_0 = N_c e^{1.24/\alpha} .$$

Having an estimate of the number distribution in the form of an exponential enables us to determine the distribution of mass

with particle diameter.

$$(5.1) \qquad m(x) = N(x)\,\frac{4}{3}\pi\left(\frac{x}{2}\right)^3\rho = \frac{1}{6}\pi\rho\,\frac{N_0}{\alpha}\,x^3 e^{-x/\alpha}$$

$$= 1.1\,\frac{N_0}{\alpha}\,x^3 e^{-x/\alpha} .$$

(ρ for sea-salt is 2.20 g/cm^3 -- Twomey (1954)) .

Figure 5.7 shows $m(x)$ versus x for $\alpha = .65$, $N_0 = 5000$. The curve has a maxima at 3α, the diameter of maximum mass. The particle diameter 3α was in the size range counted for all but six samples in this study.

The distribution of mass is, strictly speaking, only known for particles with diameter $> 1.24\mu$. We could integrate the curve between 1.24 and ∞ to obtain an estimate of the mass of ASSP in that region. However, the curve of Figure 5.6 can be integrated between 0 and ∞ to obtain an estimate of the total mass per liter of ASSP of all sizes. When we integrate the mass distribution curve of Figure 5.7 between 0 and ∞ we include the mass of particles smaller than 1.24μ, which were not counted. The contribution to the total mass of the particles in this region is small as shown by the shaded portion of the curve in Figure 5.7. Little error will be made in an estimate of total mass due to estimating the actual mass distribution curve below 1.24μ by the curve of Figure 5.7. The actual mass distribution curve cannot differ

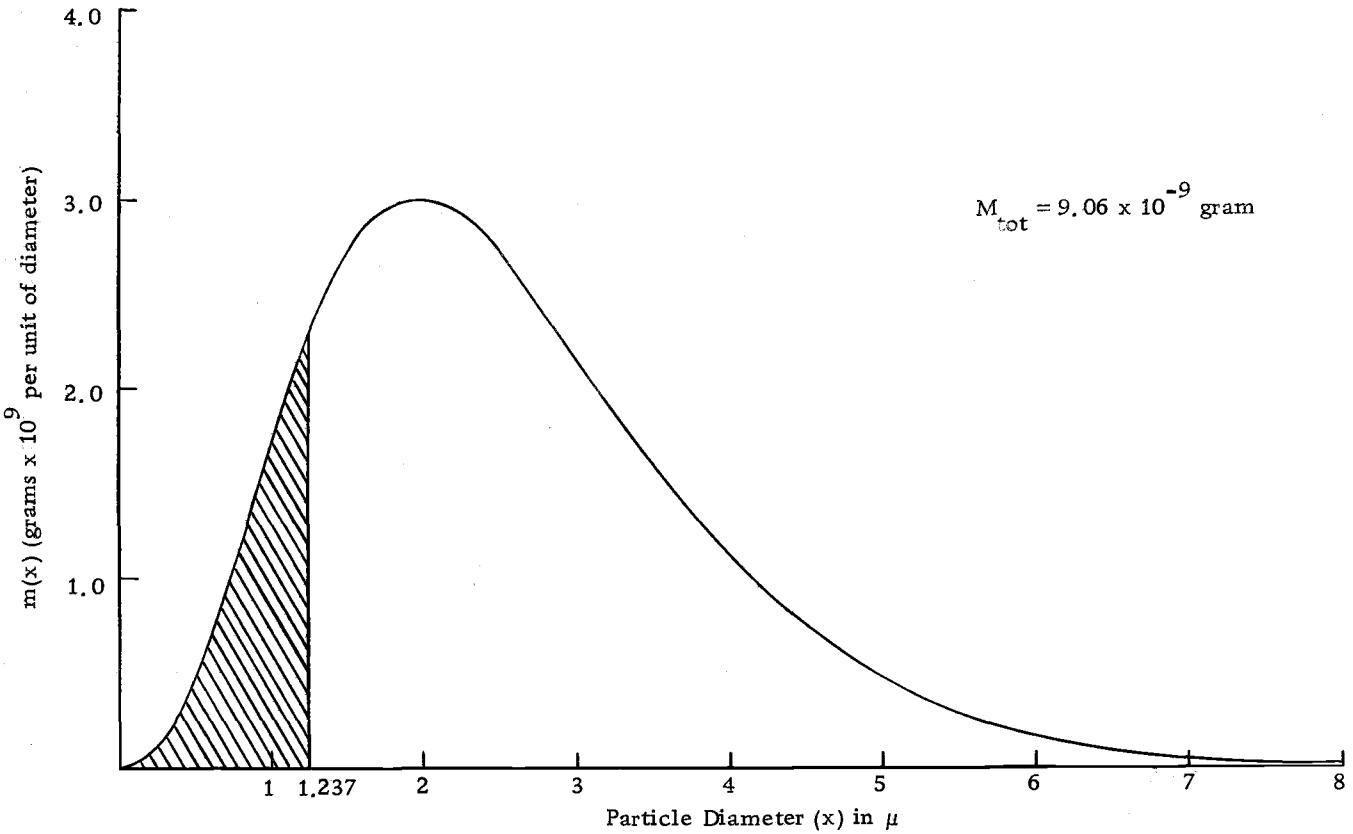

Figure 5.7. Plot of equation 5.1 showing the shape of the mass distribution curve for $\alpha = .65$, $N_o = 5000$.

greatly from that of Figure 5.7 because no matter what its shape it must merge with this curve at $x = 1.24\mu$ and it should approach zero as x approaches zero.

The total mass of ASSP is then:

$$M_{tot} = \int_0^\infty 1.1 \frac{N_0}{\alpha} x^3 e^{x/\alpha} dx = 6.60\, N_0 \alpha^3 .$$

Total mass of ASSP was computed by this formula and the values obtained are presented in Table 5.1.

It is of interest to examine the extent to which the fitted exponential number distribution can be extended to particles smaller than 1.24μ diameter. (This was the smallest size counted on the Zeiss analyzer.)

The exponential density is definitely an underestimate in the Aitken particle ($d < .2\mu$) size range. A typical Aitken particle concentration is a few hundred per cubic centimeter, many times the highest estimate of N_0 (18 per c.c.) found in this study.

The exponential is valid, however, for some ASSP in the large size range. An experiment was carried out to determine the validity of using some of the fitted exponential curves for predicting concentrations of ASSP smaller than 1.24μ diameter. Eight filters were analyzed by counting the reaction halos directly through the microscope. The technique is similar to that used in the microscopic counting of blood cells or bacteria. The operator selects

a number of microscope fields at random around the filter and counts all the reaction halos that can be seen. No attempt is made to distinguish particles as to size. An estimate is thereby obtained of the total number of ASSP per liter that can be seen by the operator. The size of the smallest particle counted by this method is .5μ, smaller than the 1.24μ diameter lower limit used on the Zeiss analyzer. The number of particles found by counting directly under the microscope should be comparable to the number predicted by integrating the fitted exponential curve over the size range counted.

Table 5.5 compares the total concentration of ASSP above .5μ in diameter found by counting under the microscope with the concentration predicted by the fitted exponential curves.

Table 5.5. Concentration of ASSP with $d > .5\mu$ found by direct count compared to the number predicted by extrapolating the exponential distribution.

Filter No.	By Direct Count	From Fitted Curve	% Difference
1	337	314	7.1
4*	691	1110	46.5
5*	819	1100	29.3
6	4570	4180	8.9
7	4100	3520	15.2
8	738	780	5.5
18*	2960	2660	10.7
41*	5060	2840	56.2

* Indicates a sample taken inland within 8 km of the beach.

The concentrations predicted by the extrapolated exponential distribution do not differ significantly from the direct counts except for filters no. 4 and 41. These two filters and also filters no. 5 and 18 were exposed inland within eight kilometers of the beach and are not well-fitted by the exponential in the size range $d > 1.24\mu$; hence it is not surprising that the extrapolated exponential is a poor estimate of the size range $d > .5\mu$ for these filters.

For cases where the exponential distribution is a good fit to the data for $d > 1.24\mu$, the exponential can be extrapolated back to $.5\mu$ to get an estimate of particles in this size range. This conclusion is tentative because only four filters from the group that were well-fitted by an exponential were involved in this comparison.

Estimate of Errors

The error involved in estimating α, N_0, total mass and the number of giant particles was checked using the data from filter number eight which was photographed and analyzed more carefully than the other filters in this study. Seventy-seven prints were analyzed to arrive at $\hat{\alpha} = .64568$ and $\hat{N}_0 = 1693$. Seventy-two of these prints were divided into eight groups of nine prints each and separate estimates of α and N_0 were made from each group. Each estimate was based on counting about the same number of particles as was counted on the other filters in this study. From

each $\hat{\alpha}$ and $\hat{N}_0$ total mass, number of giant particles, and number of particles in the size range actually counted were computed. Table 5.6 gives the results of the eight independent determinations.

Table 5.6. Results of eight separate determinations of the fitted exponential parameters from the same filter.

Replicate No.	$\hat{\alpha}$	$\hat{N}_0$	M_{tot}	$N_0 e^{-1.237/\alpha}$	$N_0 e^{-2/\alpha}$
Filter #8	.64568	1693.00	3.006	247.2	76.41
1	.63918	1834.9	3.161	264.9	80.22
2	.75436	1273.9	3.608	247.1	90.00
3	.62066	1824.5	2.878	248.6	72.80
4	.58237	1882.0	2.452	224.9	60.69
5	.54828	2218.4	2.412	232.3	57.68
6	.59246	1982.3	2.719	245.6	67.83
7	.70146	1424.3	3.243	244.1	82.32
8	.64711	1811.9	3.239	267.8	82.45
Σx	5.08588	14,252.2	23.712	1975.3	593.99
$\bar{x}$	.63574	1781.5	2.964	246.9	74.25
s	.06669	300.52	.421	14.49	11.451
$\frac{1.895s}{\sqrt{n}}(n=1)$	.126	569	.798	27.4	21.7
$\frac{1.895s}{\mu}x100\%$	19.5%	33.5%	26.5%	11.0%	28.4%
		$t_{.10}(7\text{ d.f.}) = 1.895$			

From these repeated determinations we can compute a sample variance and standard deviation for each quantity. Making the approximation that the repeated determinations are normally

distributed, we can form an approximate 90% confidence interval for a single determination of α, N_0, M_{tot}, $N_{2.0}$, and $N_{1.237}$. Table 5.6 gives the confidence intervals obtained in this way in percentage of the population mean. The percentage spread of these confidence intervals about the population means can be taken as a rough estimate of the percentage spread in confidence intervals for quantities estimated from the other filters in this study. Thus the population value of α will be within about 20% of the estimate of α unless an unlucky 1 in 10 chance has occurred. Similarly estimates of N_0 are within $\pm$ 33%, total mass $\pm$ 26%, number of giant particles $\pm$ 28%, and number of particles in the size range counted $\pm$ 11% of the estimate.

The standard deviation in percent of the mean is less for the category number of particles in the size range actually counted, than for the other categories. The reason for this is that the number actually counted does not have any error due to estimating parameters, whereas the others do include this error. This category includes only error due to counting and sampling microscope fields around a filter.

Presentation of Inland Profiles

The quantities which were examined with distance inland are: (1) the total mass of ASSP; (2) the concentration of ASSP with diameter greater than two, three, and four micrometers; (3) the number of particles in the size range that was actually counted ($d > 1.237\mu$). For the data which was well-described by an exponential density, these quantities were taken from the fitted exponential curves, but for the data collected inland within eight kilometers of the shoreline, these quantities were estimated from the raw data. As a result of using the raw data for the inland nearshore samples, the estimates of total mass will probably be slight underestimates, since particles smaller than 1.24μ diameter are not included. The total mass contributed by all particles with diameter less than 1.24μ is small compared to the mass of all the larger particles. Figure 5.7 shows approximately the fraction of mass that is being left out (shaded portion of the area under the curve).

The inland profile data were obtained from 49 samples collected on three separate days. The data of July 14, 1971 is the best because of the greater number of data points and because each station was sampled about five times.

Figure 6.1 shows the total mass of ASSP versus distance inland from Newport, Oregon for the three days that inland profiles were

taken. Where more than one sample was taken at a station on a given day the concentration is the average of the values obtained at the different times. The total mass of ASSP drops off very sharply in the first two to five kilometers from the beach and then decreases at a relatively slower rate from there inland. Figure 6.2 shows the variation of giant ASSP with distance inland for the three days sampled. The shape of the profile of giant ASSP is similar to the shape of the total mass profile.

Figures 6.3, 6.4, and 6.5 show the average concentration of various size particles versus distance inland for the three days--July 14, 1971; April 16, 1971; and December 22, 1970. The ordinate is logarithmic because of the wide differences in concentration. The curve for $d > 1.237\mu$ is put in because this was the particle range that was actually counted. The values for this curve are obtained from direct counts, not from the fitted distribution curves. Figure 6.3 also shows the elevation above sea level of the route along which the samples were taken.

Figure 6.6 is the individual determinations of giant ASSP with distance inland for July 14, 1971. The profile obtained earliest in the day showed the lowest concentrations and the level of ASSP more or

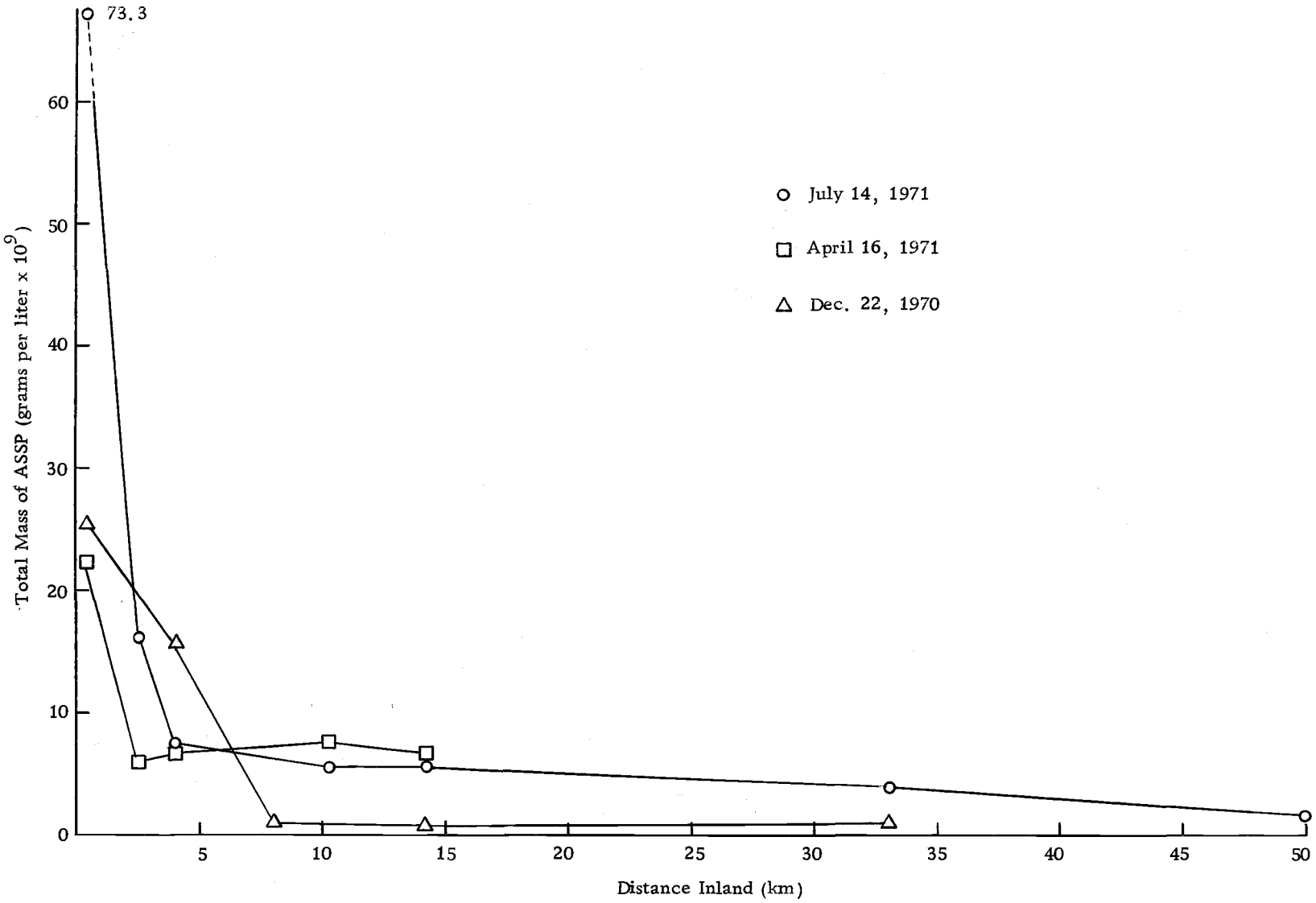

Figure 6.1. Total mass of ASSP versus distance inland for the three days indicated.

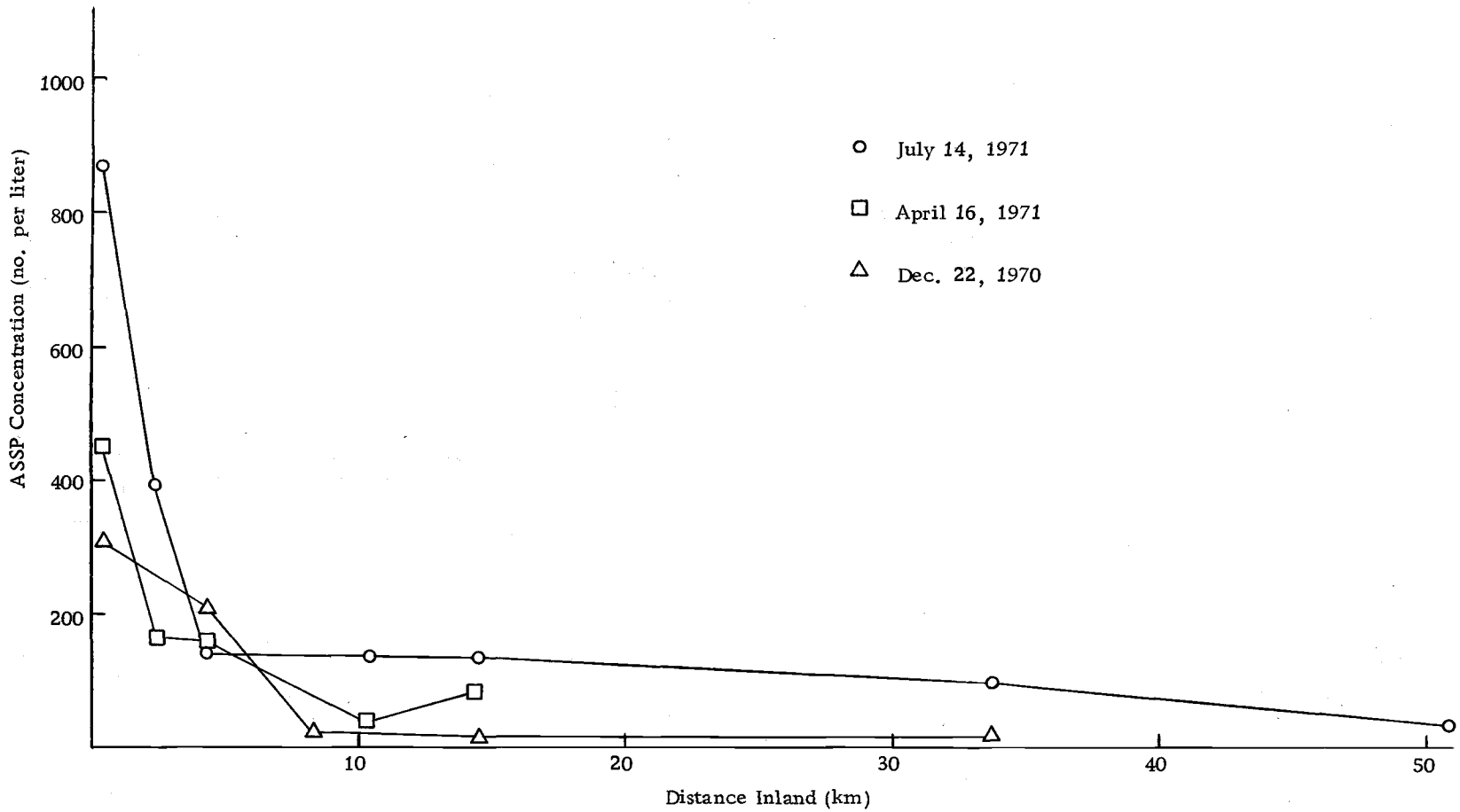

Figure 6.2. Number of giant ASSP per liter versus distance inland for the three days indicated.

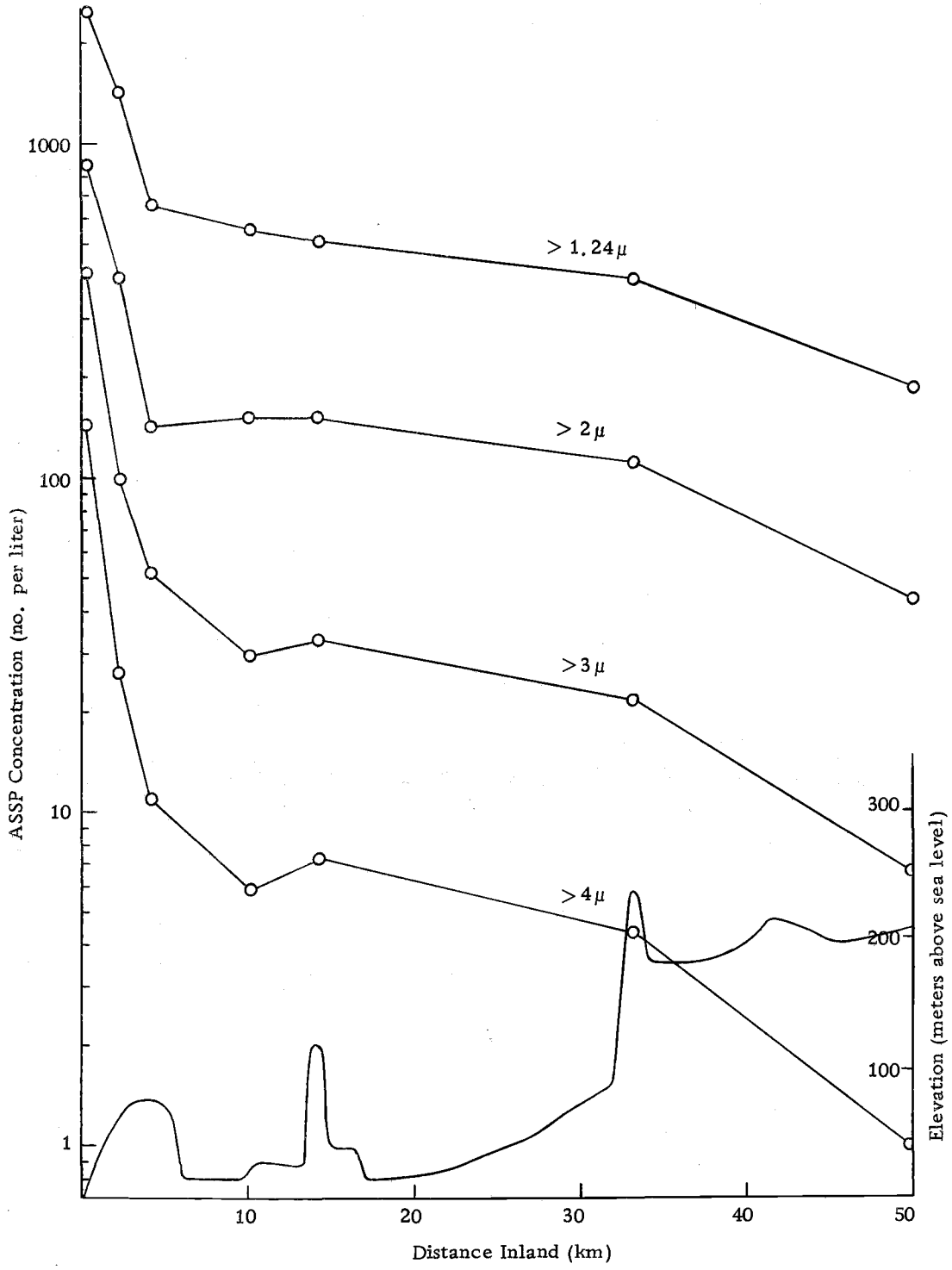

Figure 6.3. Average ASSP concentration versus distance inland for data of July 14, 1971. Also elevation above sea level along the sampling route is shown.

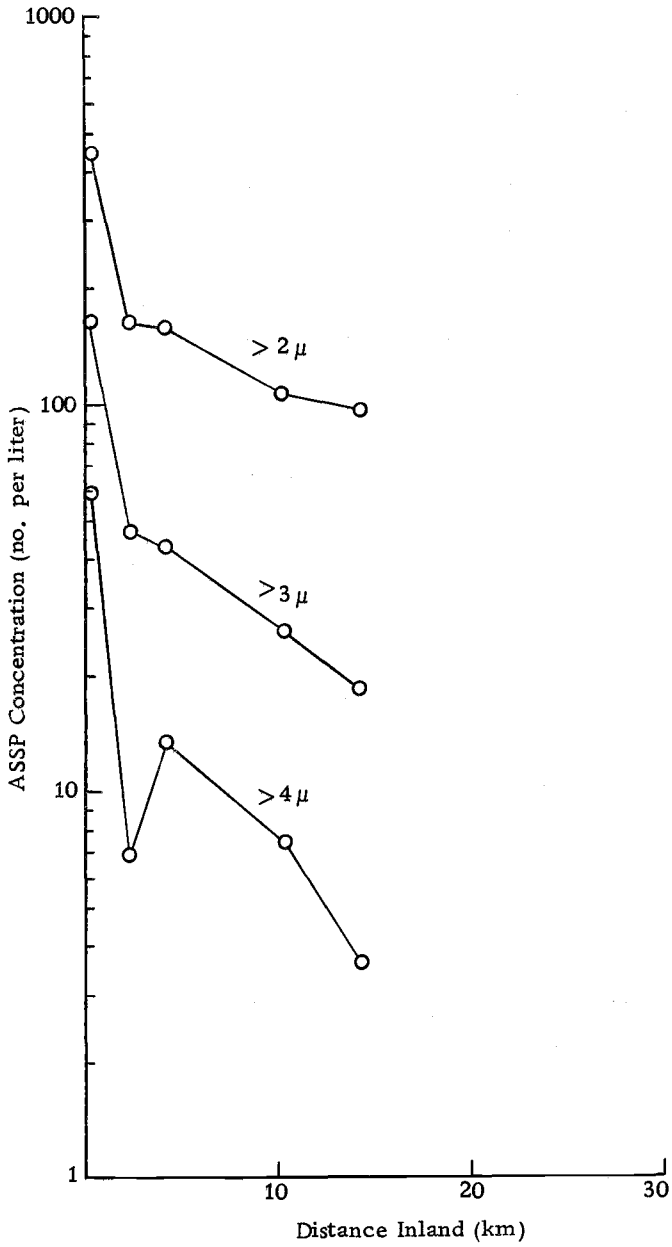

Figure 6.4. Average ASSP concentration versus distance inland for data of April 16, 1971.

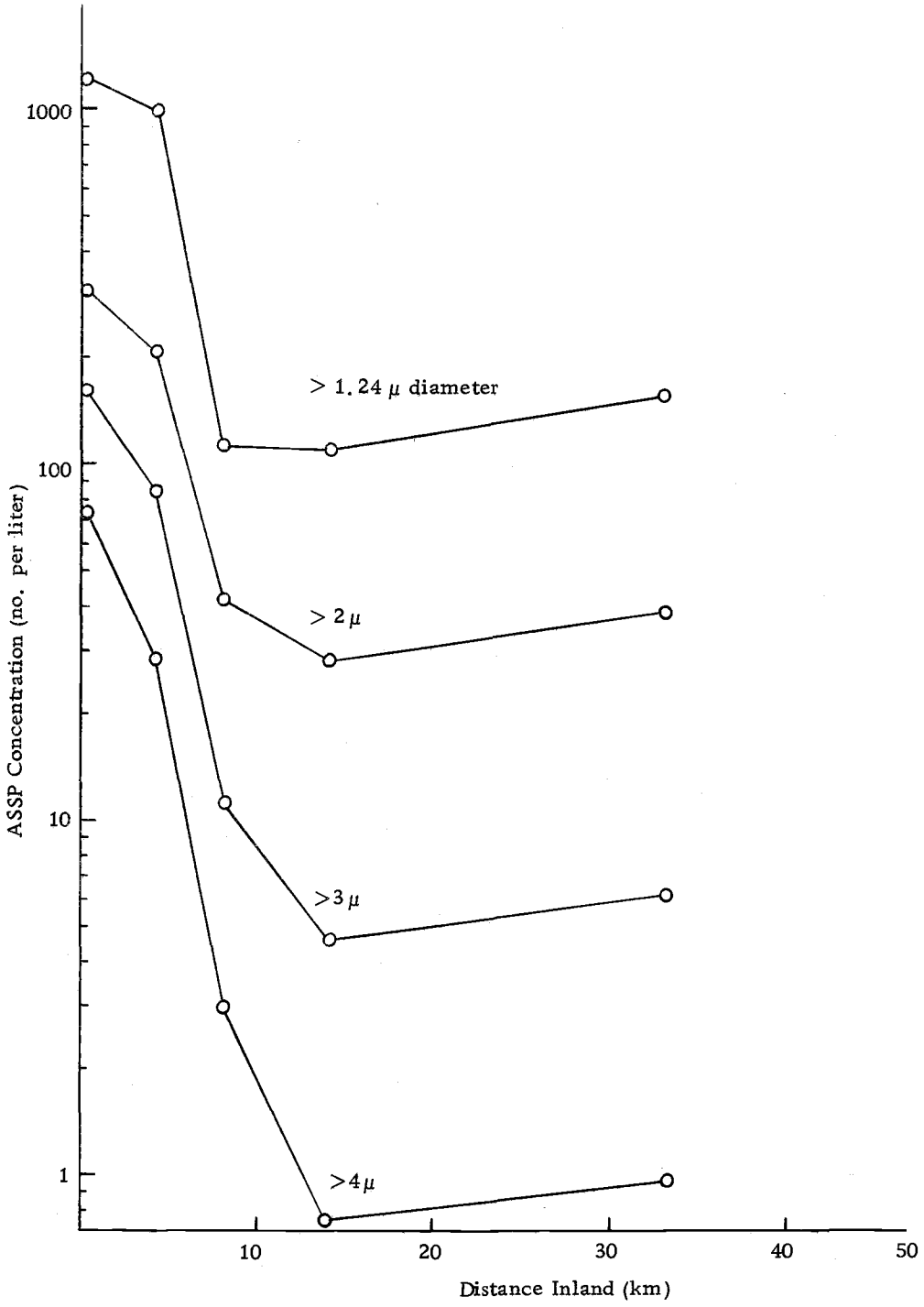

Figure 6.5. ASSP concentration versus distance inland for data of Dec. 22, 1970.

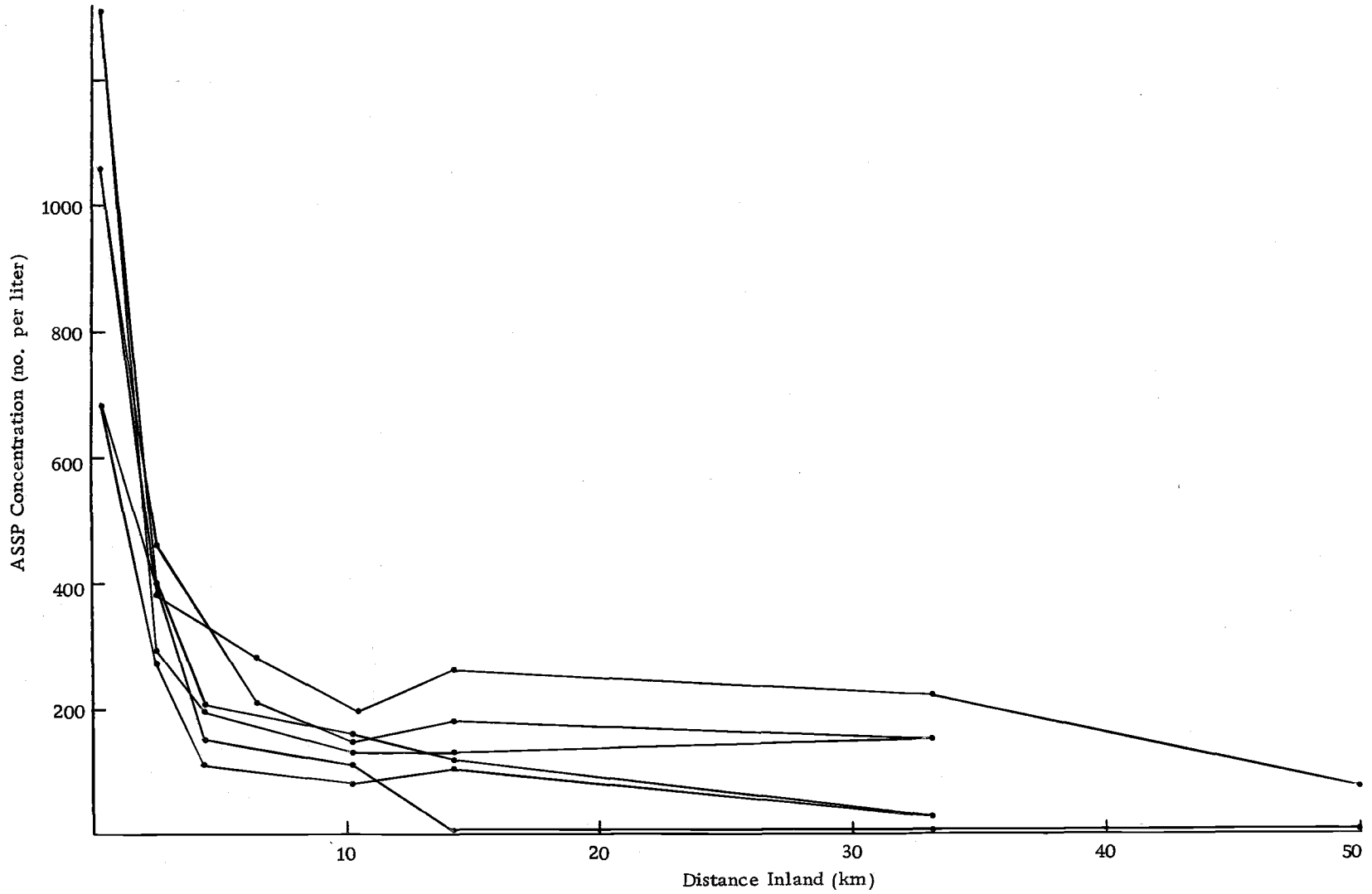

Figure 6.6 Individual giant ASSP profiles of July 14, 1971.

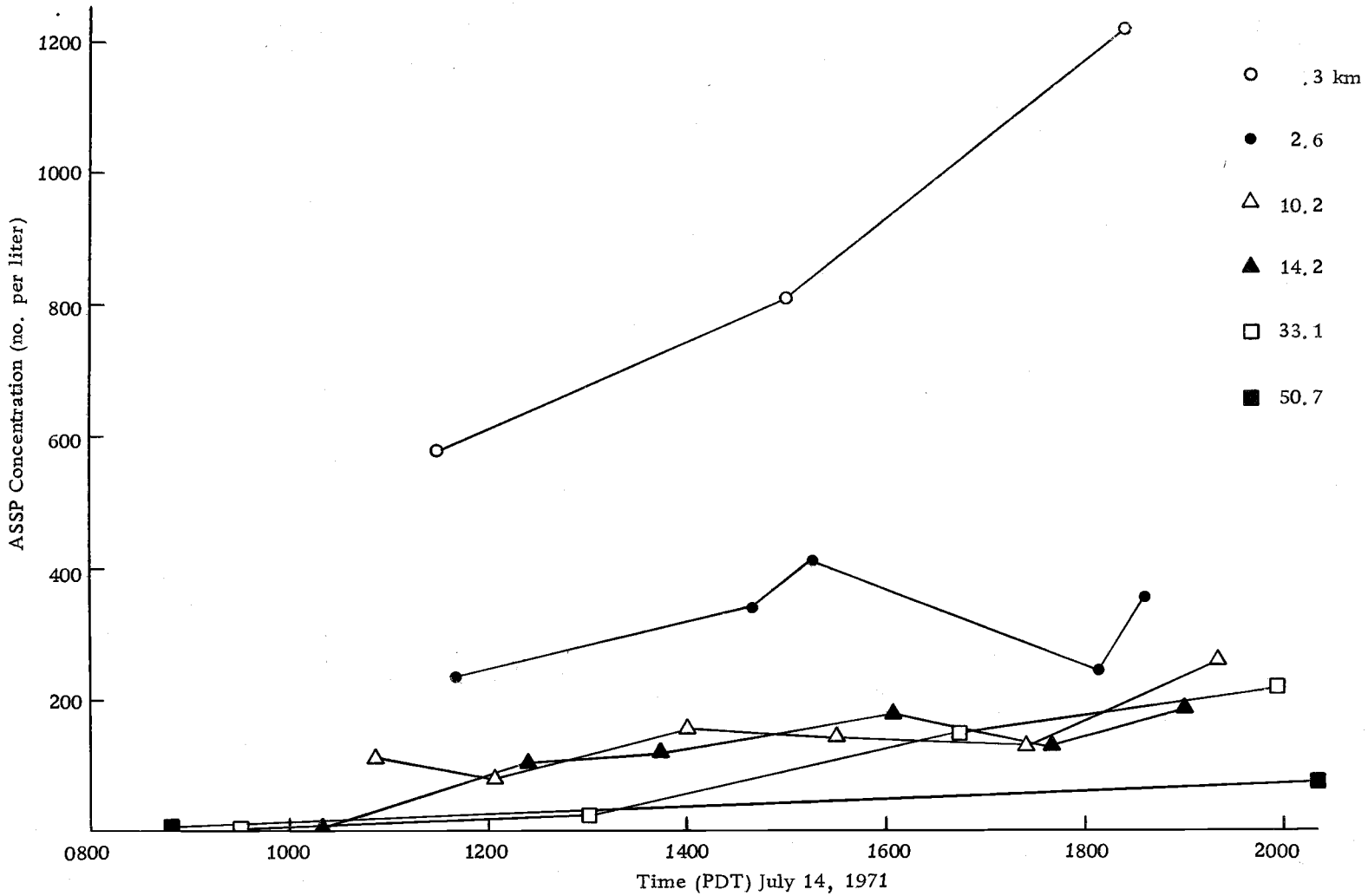

Figure 6.7. Giant ASSP concentration versus time for data of July 14, 1971.

less increased during the day. Figure 6.7 shows the variation with time of the giant ASSP data for July 14, 1971.

The total mass profiles of Figure 6.1 demonstrate the great amount of deposition of sea-salt that must occur in coastal areas. This salt deposition causes fast oxidation of metals and paint. From this point of view it is interesting to note from Figure 6.1 that most of the sea-salt mass is deposited within eight kilometers of the shoreline. Further inland than eight kilometers the total mass of ASSP present in the air decreases quite slowly with increasing distance inland, implying a small deposition of sea-salt mass.

The Fit to Tanaka's Model

The data provided an opportunity to test the theoretical model of the inland distribution of giant ASSP developed by Toba and Tanaka between 1961 and 1965 and presented in exact form by Tanaka (1966). In this model the inland distribution of giant ASSP is estimated on the basis of diffusion theory. The vertical distribution of ASSP over the ocean is taken to be an exponential decrease with height, based on the observations of Woodcock (1953, 1957, etc.) and Lodge (1955). Wind speed and eddy diffusivity are assumed constant. It is also assumed that an onshore wind brings inland a steady supply of particles and

that particles are lost on land by gravitational fallout and impaction on ground obstacles. The effect of impaction on ground obstacles is expressed by an efficiency of impaction, λ.

The equation is

$$u\frac{\partial\theta}{\partial x} = w\frac{\partial\theta}{\partial z} + D\frac{\partial^2\theta}{\partial z^2} \tag{6.1}$$

where θ = number concentration of a given size particle

x = horizontal distance inland

z = height above the ground

u = uniform wind speed (assumed onshore)

w = particle settling velocity

D = eddy diffusivity

The boundary conditions are

$$\theta = 0 \ @ \ z = \infty \tag{6.2}$$

$$\theta = \theta_{00}\exp(-\frac{w}{D}z) \ @ \ x = 0 \tag{6.3}$$

$$D\frac{\partial\theta}{\theta z} = \lambda\mu\theta \ @ \ z = 0 \ . \tag{6.4}$$

Condition 6.2 simply requires that the concentration approach zero at far inland points. 6.3 is the condition that the vertical distribution at the coast be of the exponential form suggested by Toba (1965). θ_{00} is the concentration at $z=0$ and $x=0$. Equation 6.4 defines λ, the efficiency of impaction. $(D\frac{\partial\theta}{\partial z})_{z=0}$ is the downward flux due to the

vertical gradient of particle concentration. Equation 6.4 says that this downward flux must equal the particles lost by impaction, expressed as $\lambda_u \theta_0$. Since only a portion of the particles which diffuse downward to near ground level impact, λ is introduced to take account of the effect.

Following Tanaka, we introduce dimensionless parameters Φ, ξ, ζ, and γ defined by

$$\Phi = \frac{\theta}{\theta_{00}}, \qquad \xi = \frac{w^2 x}{4Du}, \qquad \zeta = \frac{wz}{2D}, \text{ and } \gamma = \frac{\lambda u}{w}.$$

Φ is the dimensionless number concentration of ASSP scaled by θ_{00}--the ground level concentration at the coast. ξ is proportional to the distance inland with scaling factor $\frac{w^2}{4Du}$. ζ is the dimensionless distance above the ground scaled by $\frac{w}{2D}$. γ is the ratio between the ground sink due to the impaction by ground obstacles and that due to the sedimentation of the particles, and Tanaka calls it the impaction to sedimentation ratio.

The solution of the equation under these boundary conditions is

$$(6.5)\quad \Phi(\xi, \zeta) = \frac{1}{2}\operatorname{erfc}\left(\sqrt{\xi} - \frac{\zeta}{2\sqrt{\xi}}\right) e^{-2\zeta} - \frac{1}{2}\left(1 + \frac{1}{\gamma}\right)\operatorname{erfc}\left(\sqrt{\xi} + \frac{\zeta}{2\sqrt{\xi}}\right)$$

$$+\left(1 + \frac{1}{2\gamma}\right) e^{2\gamma\{\zeta + 2(1+\gamma)\xi\}} \operatorname{erfc}\left\{(1+2\gamma)\sqrt{\xi} + \frac{\zeta}{2\sqrt{\xi}}\right\}.$$

Since the data for this study were surface observations, we need only the solution for $\zeta = 0$.

$$(6.6)\quad \Phi_0(\xi) = (1 + \frac{1}{2\gamma})e^{4\gamma(1+\gamma)\xi}\ \mathrm{erfc}\{(1+2\gamma)\sqrt{\xi}\} - \frac{1}{2\gamma}\ \mathrm{erfc}(\sqrt{\xi}).$$

This equation for the inland surface distribution of ASSP was compared with the raw data collected July 14, 1971 for particle classes 3, 5, 7, 9, and 11. Since the solution (eq. 6.6) is for one particle size only, the size classes were represented by the midpoint of the diameter range. The average onshore wind speed and relative humidity were taken from observations made while sampling to be 3m/sec and 70% respectively. γ, the impaction to sedimentation ratio, and D, the eddy diffusivity, are not known. Tanaka says γ is an arbitrary constant and probably has a value between 10 and 100 based on observations of the verticle distribution of ASSP by Byers et al. (1957), Reitan and Braham (1954), Podzimek and Cernock (1961), and Meszaros (1964).

D, the eddy diffusivity, is somewhere between 10^2 and 10^6 for most meteorological conditions. Craig (1949) gives values for D at different heights for a condition of light stability. D varied from $.9 \times 10^4$ at the surface to a maximum of 30×10^4 at 70 meters and then decreased with height to $.2 \times 10^4$ at 200 meters. Since the data from this study of July 14, 1971 was collected under conditions which could be described as "light stability" it seems reasonable to use $D = 10^4$ as a starting point for fitting the model to the data.

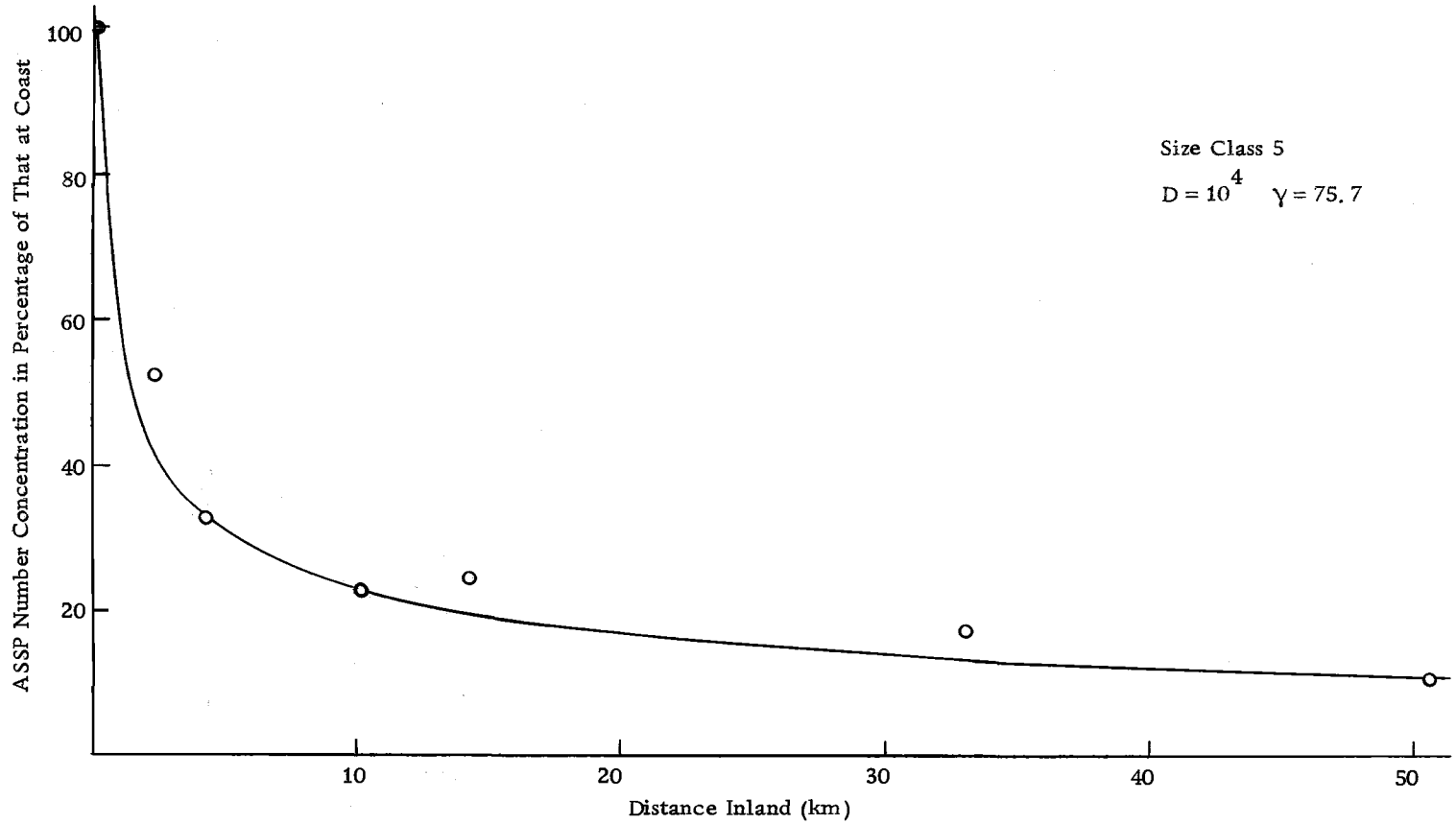

Figure 6.8. Inland distribution of ASSP. Size class 5 data compared to the fitted model.

D was set at 10^4 and γ was left to be determined by the data. A fit to the data was obtained by requiring equation (6.6) to give the observed concentration of ASSP of size class five at the 10.2 km station. γ is thereby fixed to be 75.7. Figure 6.8 shows the fit of equation 6.6 to the time averaged data of July 14, 1971 for size class five. Note that the concentration at the 14 km station is actually higher than that at the 10.2 km situation. It is believed that this is due to the fact that the 14 km station is on a low coastal mountain of elevation 115 meters while the 10.2 km station is near sea level. Tanaka's model predicts an increase of concentration with height for inland points and Byers, Sievers, and Tufts (1957) have observed this effect.

In the model the increase of particle concentration with height is caused by the large ground sink due to impaction. At the coast ($\xi = 0$) there is no increase with height; further inland the model predicts that the maximum ASSP concentration occurs at a progressively higher altitude. Equation 6.5 which includes the vertical distance parameter ζ, can be used to predict the concentration inland at some height above the ground. If we apply this equation to the 14 km station, putting in the altitude as 115 meters, we find a concentration of .712 of that at the coast, much greater than the .244 observed. The effect of an increase with height was observed on the

mountain, but not as much as was predicted by the model if the observation had been 115 meters above the earth's surface. As the air moves over a mountain there is increased mixing of upper air with surface air due to the increased surface friction. The surface layer of air tends to lag as it climbs the mountain slope, causing greater shear with upper layers and hence increased mixing with upper air. Equation 6.5 then is not applicable to this case--it would apply if the measurement were taken 115 meters above the (flat) ground surface. The anomaly between the station at 10.2 km and the station at 14 km is explained qualitatively at least by Tanaka's model. The mountain station was getting some of the upper level air that contained a higher concentration of ASSP.

The station at 33 km inland is also a low coastal mountain pass of elevation 235 meters. The values $D = 10^4$ and $\gamma = 75.7$ are not the only ones which give a reasonably good fit to this data. It was found that if D was set at 10^5, a good fit could be obtained with $\gamma = 265$. $D = 10^3$ and $\gamma = 25$ also gave a fit about as good as that obtained with $D = 10^4$, $\gamma = 75.7$. D and γ cannot be determined from the data in this study, but if a value for D is chosen, then there is only one γ that will give a reasonable fit to the data. $D = 10^5$ is too large, since $\gamma = 265$ does not agree with Tanaka's statement that γ is between 10 and 100. $D = 10^3$ is too small for the weather conditions that prevailed.

Using $D = 10^4$ and $\gamma = 75.7$ the fit of equation (6.6) to other sizes of ASSP was examined. Figures 6.9, 6.10, and 6.11 show the fit of equation (6.6) to the data for size classes 7, 9, and 11 respectively. The fit for size classes 7, 9, and 11 is remarkably good, especially considering that the values of D and γ that gave this fit were originally obtained from data on particles of size class 5.

When an attempt was made to fit particles of size class three ($1.24 \leq d \leq 1.62\mu$) the fit of the data to equation (6.6) was not so good (see Figure 6.12). The predicted values are mostly too high by about 50%. It is not possible to account for this discrepency by errors in computing the droplet diameter or settling velocity. Nor is the poor fit due to inaccurate counting of size class three particles, for the concentration at the coast was determined by the same counting procedure as the inland stations, and the inland concentrations are given as percentage of that at the coast. It could be that small particles have a different impaction ratio, γ, than large particles. An investigation by May (1945) on impaction efficiencies of different size particles indicate that γ is, if anything, <u>smaller</u> for smaller particles, so this does not explain the poor fit. It is possible that particles of size class three have become deficit in chloride ion, so that the microchemical method used to detect them, which depends on the chloride ion, gives too small a reaction spot on the filter. The assumption made in Chapter II, that all particles sampled have the

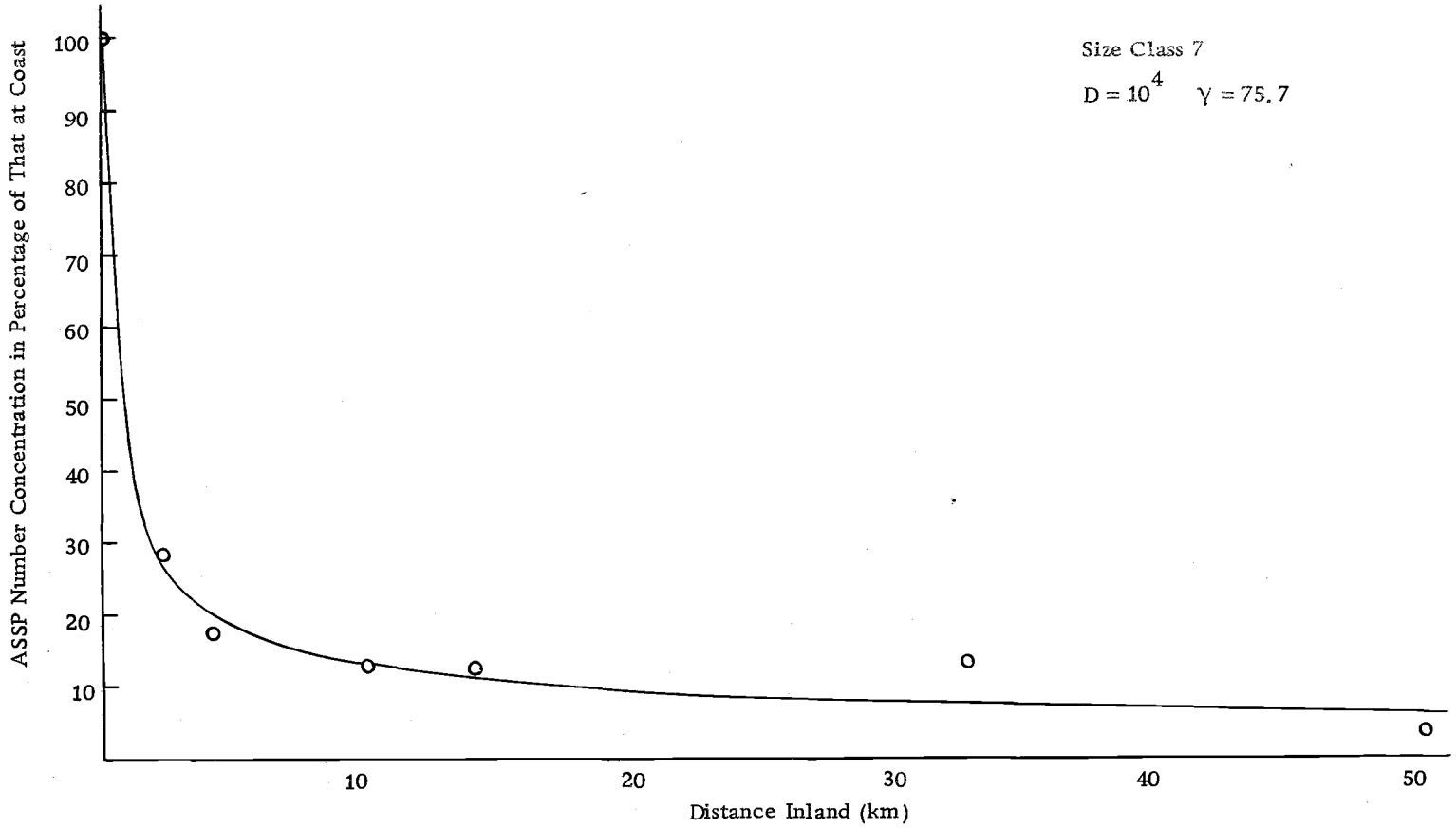

Figure 6.9. Inland distribution of ASSP. Size class 7 data compared to the fitted model.

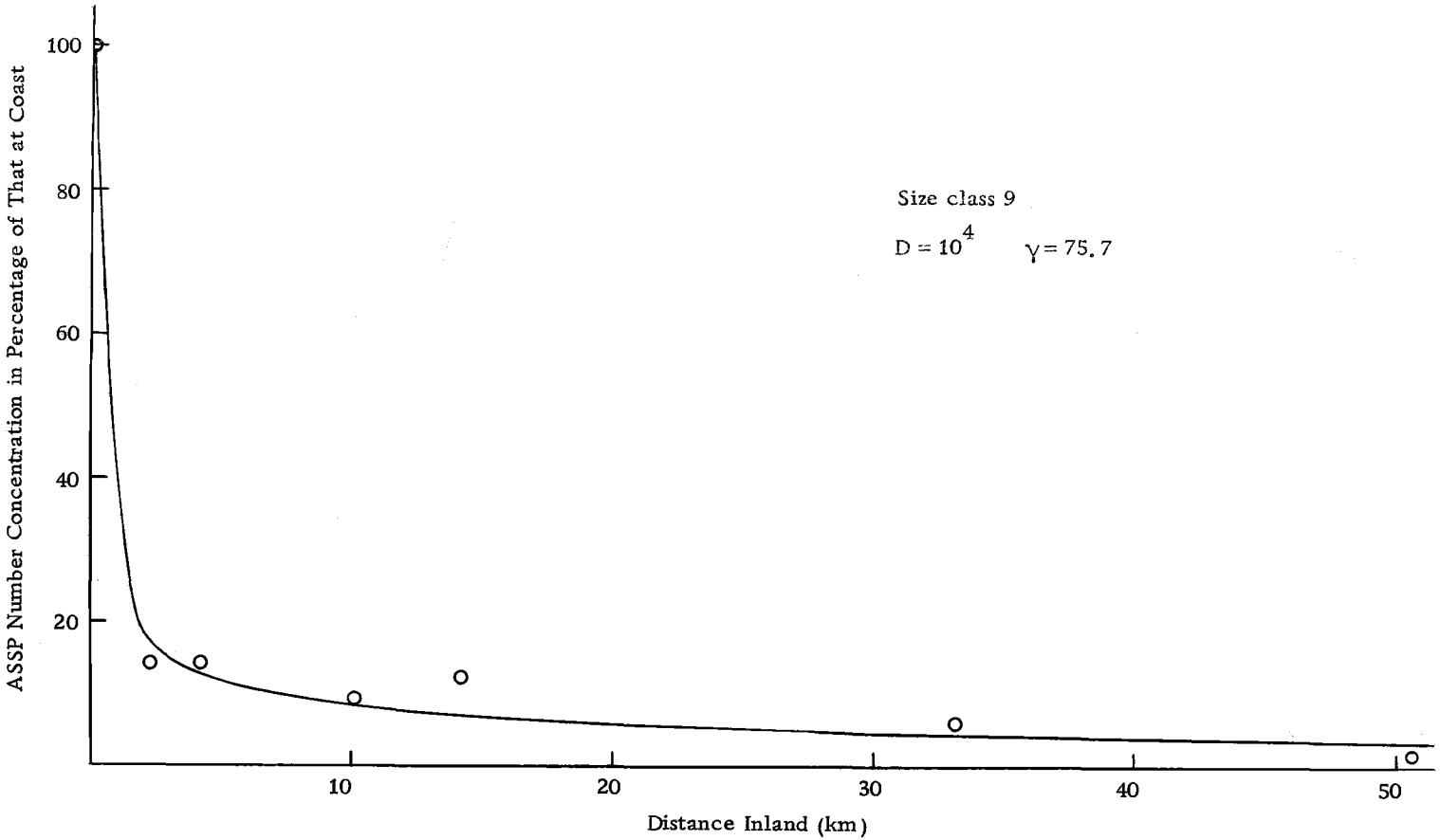

Figure 6.10. Inland distribution of ASSP. Size class 9 data compared to the model.

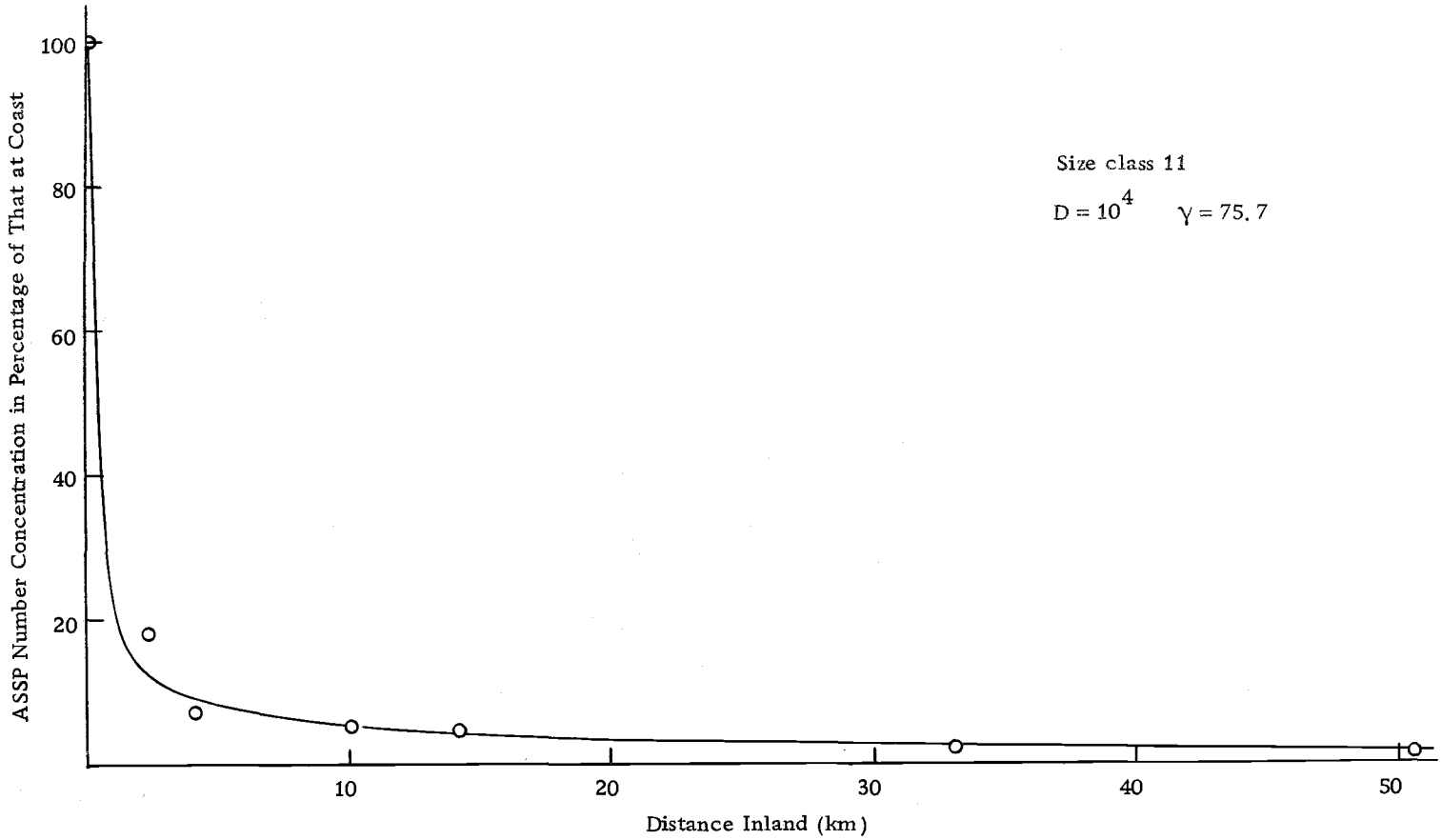

Figure 6.11. Inland distribution of ASSP. Size class 11 data compared to the model.

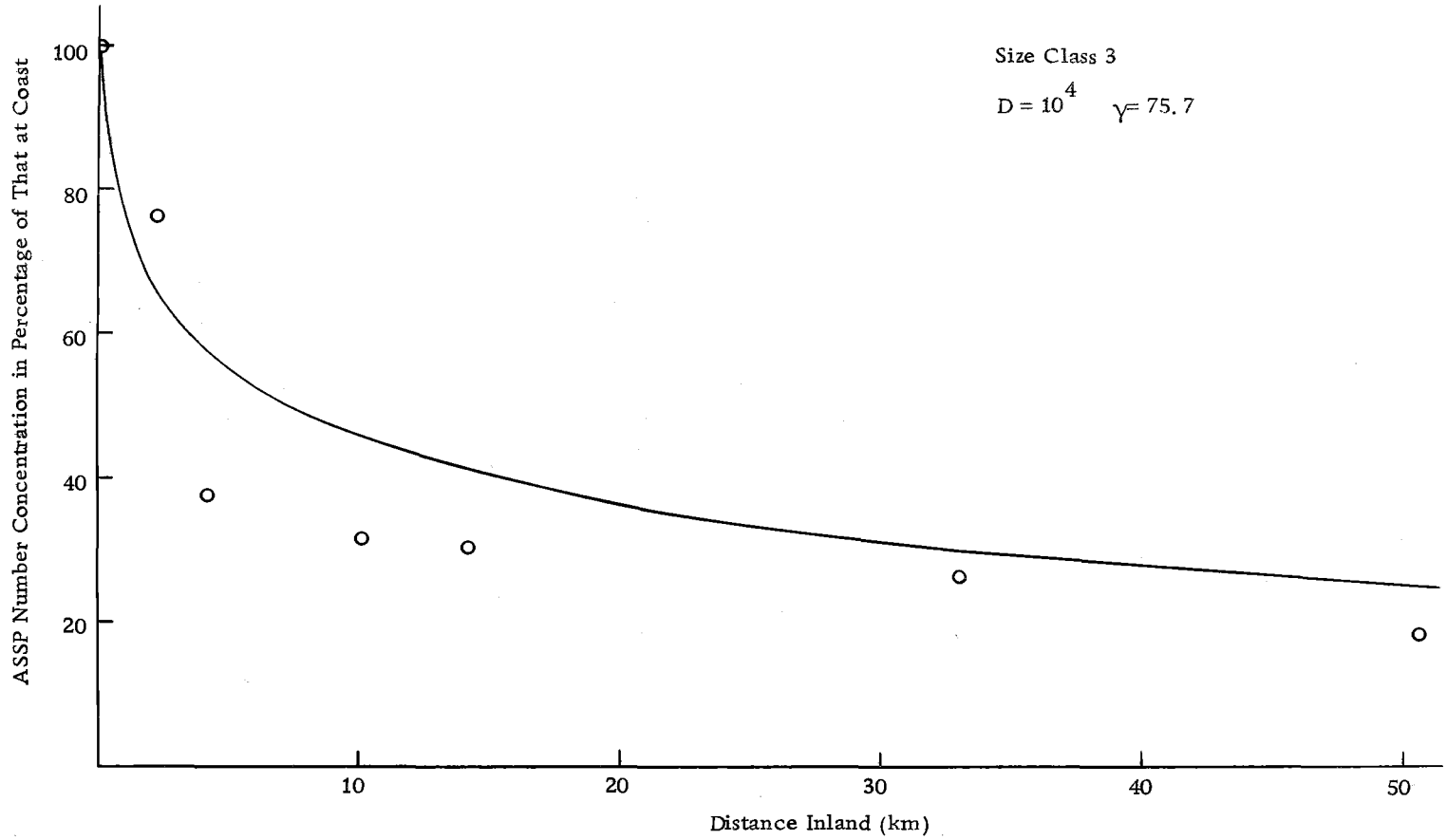

Figure 6.12. Inland distribution of ASSP. Size class 3 data compared to the model.

relative composition of sea-salt, has been found to be a good approximation for giant ASSP ($d > 2\mu$). However, for particles in the large size range there is evidence that chloride ion is lost relative to other major ions. Junge (1956) found that the $\frac{Cl}{Na}$ ratio of giant ASSP was that of sea-salt, but that large particles had a $\frac{Cl}{Na}$-ratio that was, on the averate $\frac{1}{3}$ that of sea-water. Junge (1963) summarized observations of the chemical composition of ASSP by saying that there is a release of Cl^- from ASSP relative to the other major ions but that the mechanism of this release is not clear. The chemical reaction which strips Cl^- from ASSP is not known but the postulated reactions involve reaction of the particle with gases in the air. The smaller particles lose more chloride because of their larger surface to volume ratio. The effect of this chloride loss would qualitatively explain the too low concentrations for size range three in Figure 6.12.

Apparently Toba and Tanaka have interpreted accurately the physical processes which determine the inland distribution of ASSP. It is a balance between particles supplied by advection and turbulent diffusive transport and particles lost by sedimentation and impaction on ground obstacles. It is interesting to examine the inland distribution which is predicted if there is no effect due to impaction ($\gamma = 0$). Figure 6.13 shows the inland surface distribution for size class five with $\gamma = 0$ and the curve with $\gamma = 75.7$. It should be clear from Figure 6.13 that the effect due to impaction on ground obstacles is

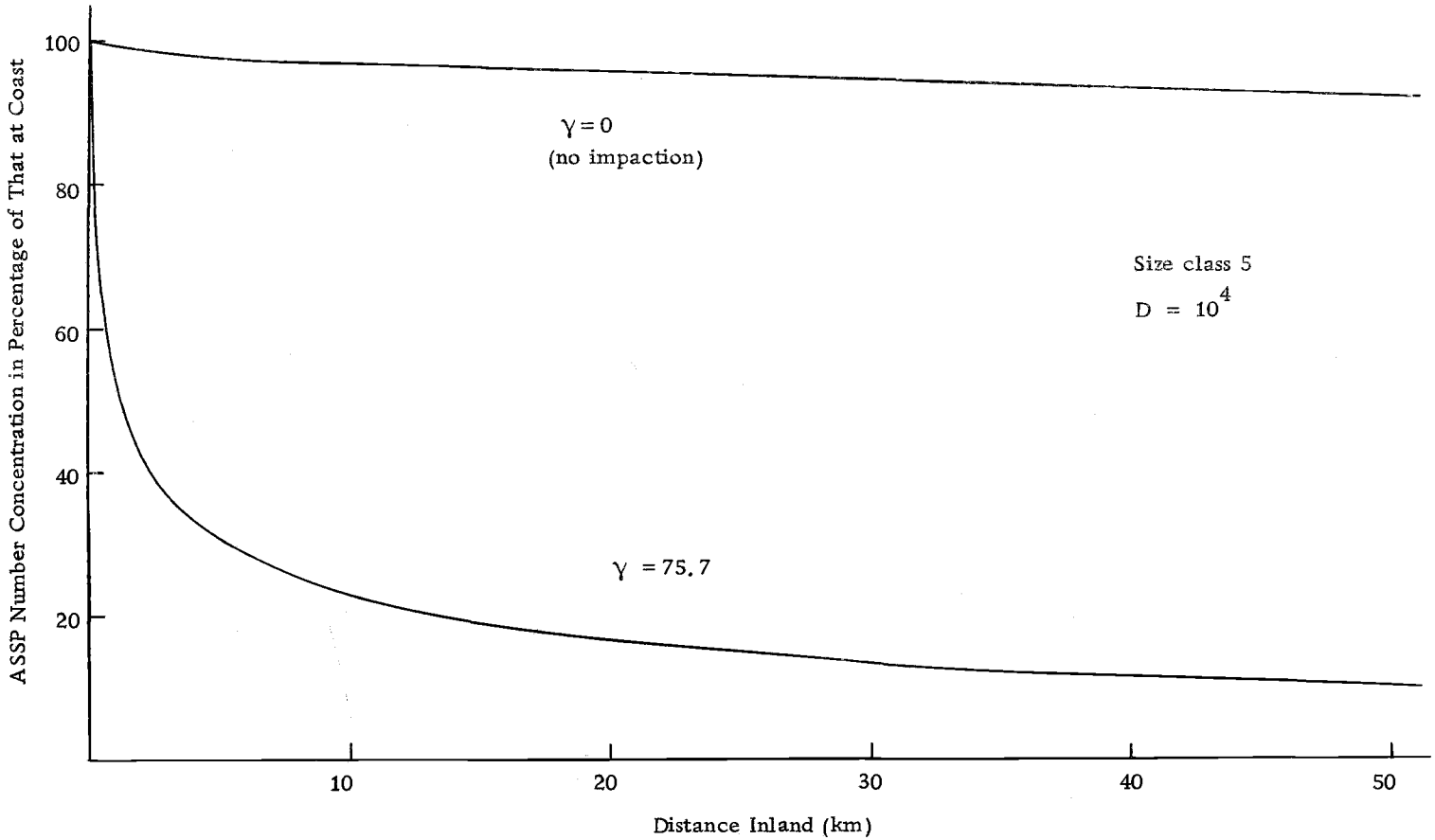

Figure 6.13. Inland distribution of ASSP for size class 5 with and without effect due to impaction on ground obstacles.

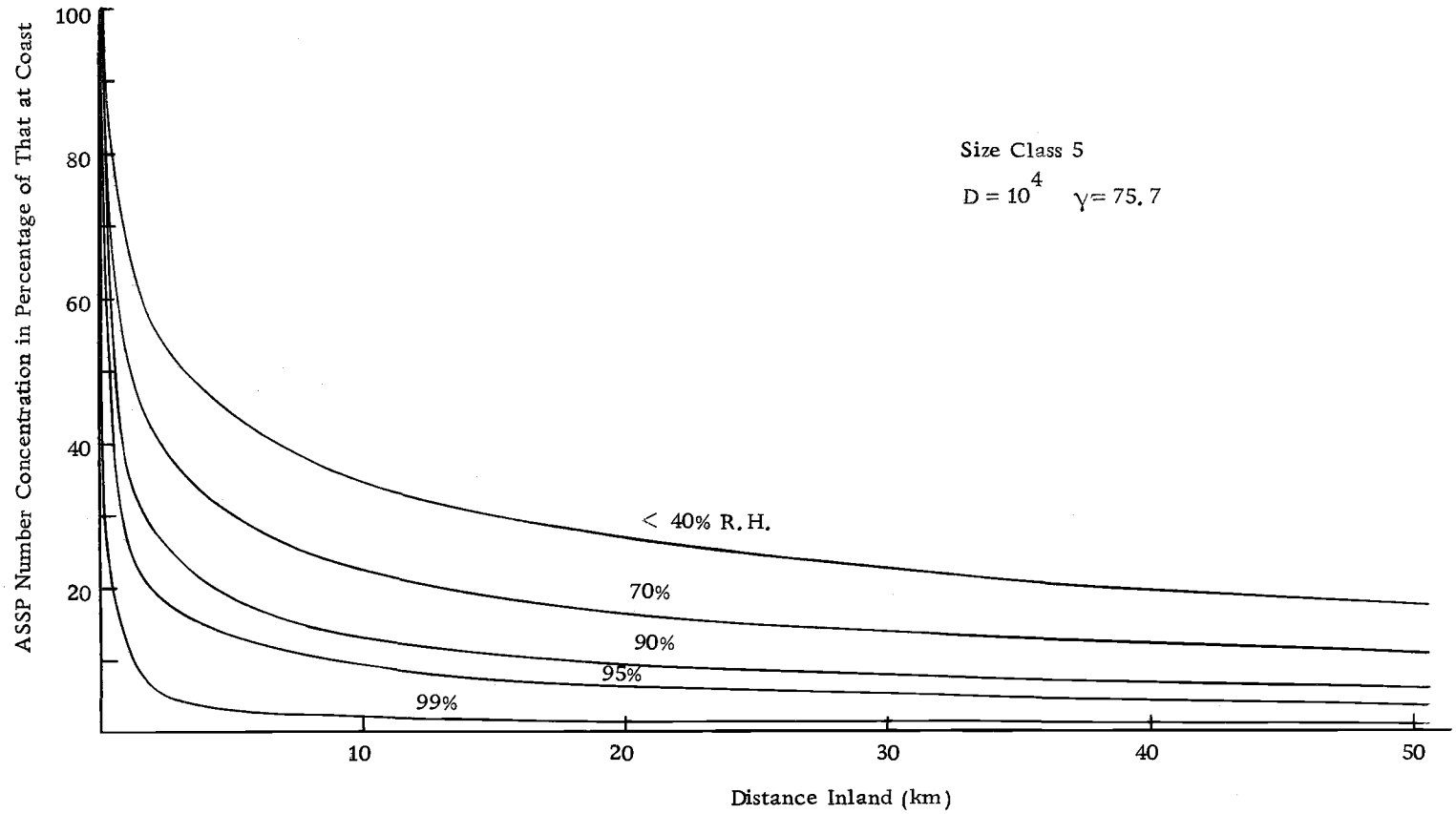

Figure 6.14. Inland distribution of ASSP predicted by the model for various relative humidities.

much greater than that due to sedimentation. λ , the impaction efficiency is increased by vegetation, especially trees whose leaves offer a large surface area for the particles to impinge upon. The terrain between Newport and Corvallis, Oregon where the measurements were taken is almost entirely covered by vegetation and about one-half covered by trees. This lends support to our value of γ of 75.7 which is towards the upper end of the scale that Tanaka has suggested.

Tanaka's model predicts that the inland distribution of ASSP is quite sensitive to the particle settling velocity, w. (w occurs squared in the formula for the inland concentration.) The settling velocity on the other hand, is sensitive to small changes in relative humidity when the humidity gets above about 85 %. Consequently, the percentage of ASSP that will penetrate inland is quite sensitive to relative humidity, for the higher humidities. Figure 6.14 shows the inland distribution predicted by the model for size range five for various relative humidities. High relative humidity will result in a great amount of sea-salt particles being deposited near the coast, whereas a dry day with an onshore wind will result in a large amount of ASSP being transported inland and deposited over a wide area inland.

Comparison with Other Inland Profiles

Few studies provide data to compare with the inland profile

data of this study. However, the work by Lodge (1955) in Puerto Rico and by Hama and Takagi (1970) in Japan are comparable in some respects.

Hama and Takagi measured total mass and number of giant ($d > 2\mu$) ASSP along the bank of the Tedori River, Japan. This river is nearly perpendicular to Mikawa beach. The wind speed was reported to be about 9 m/sec but no other weather data were provided. The inland profile of giant ASSP which they found is shown in Figure 6.15 along with the giant ASSP data from this study for July 14, 1971. Hama and Takagi took all their samples within one kilometer of the beach, making comparison with this study awkward. However, it can be seen that there is a greater dropoff of giant ASSP concentration in one kilometer in the Japanese study than was encounted in 2.3 km in this study. This significantly greater decrease found by Hama and Takagi could be due to several things besides the possibility of experimental errors in either study. One is that the wind direction was offshore or had an offshore component. In this case there is no advective inland transport and we would expect little or no inland penetration of ASSP. Another possibility, in the case that the wind had an onshore component, is that the relative humidity was much greater than the 70% humidity encountered in this study. The relative humidity which would have been necessary to explain Hama and Takagi's findings can be approximately estimated from Tanaka's model. Assuming the

onshore component of wind was the same as encountered in this study, 3 m/sec, a relative humidity of 97.5% would be necessary to give a concentration of .19 of the coastal concentration at 1 km. If the entire wind of 9 m/sec was directly onshore, a humidity of about 98.8% would be necessary to give a concentration of .19 at 1 km from the beach. If Hama and Takagi were sampling on a moist or rainy day, it would not be unusual for them to encounter humidities as high as 98%, especially at the coast. This could explain the much sharper decrease of ASSP with distance inland which they found.

Lodge (1955) made measurements of ASSP at five points inland from the beach near Ponce, Puerto Rico. He obtained data for ASSP with diameters greater than 3μ which is compared with data from this study in Figure 6.16. Lodge also found a sharp initial decrease in ASSP with a more gradual decline further inland. His point of "leveling out" (.4 km) is much closer to the beach than was found in Oregon, but is similar to the giant ASSP data of Hama and Takagi. Lodge found the point of "leveling out" to be 450 meters or .45 km from the beach.

Lodge found that the concentration of ASSP with $d > 3\mu$ at 1.3km from the beach was .20 of that at the beach. This study found the concentration of ASSP with $d > 3\mu$ was .26 of that at the beach at 2.3 km from the beach. This discrepency cannot be explained by wind direction or speed, because Lodge reports an onshore wind speed

of 4.4 m/sec. These different results could be accounted for by a higher relative humidity in Lodge's study. We can get some idea of the humidity required from Tanaka's model. For a wind speed of 4.4 m/sec and a dry particle size of 3.8μ Lodge's concentration of .20 at 1.3 km would occur if the relative humidity were 97.4%. Lodge does not say what the humidity was while he was sampling, but he does say that there was rain on at least one of the days he sampled.

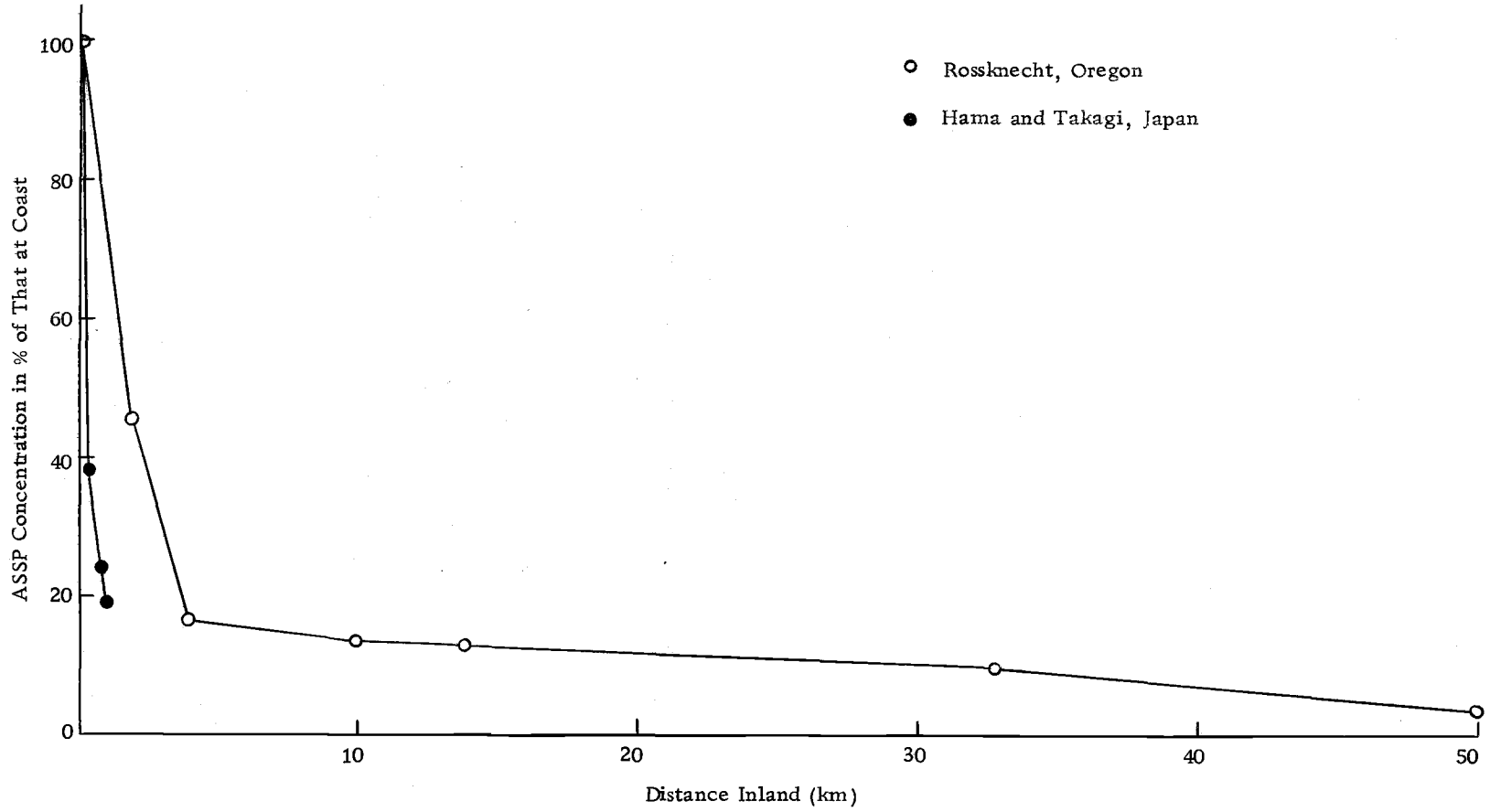

Figure 6.15. Data on Giant ASSP from this Study Compared to Data Collected by Hama and Takagi in Japan.

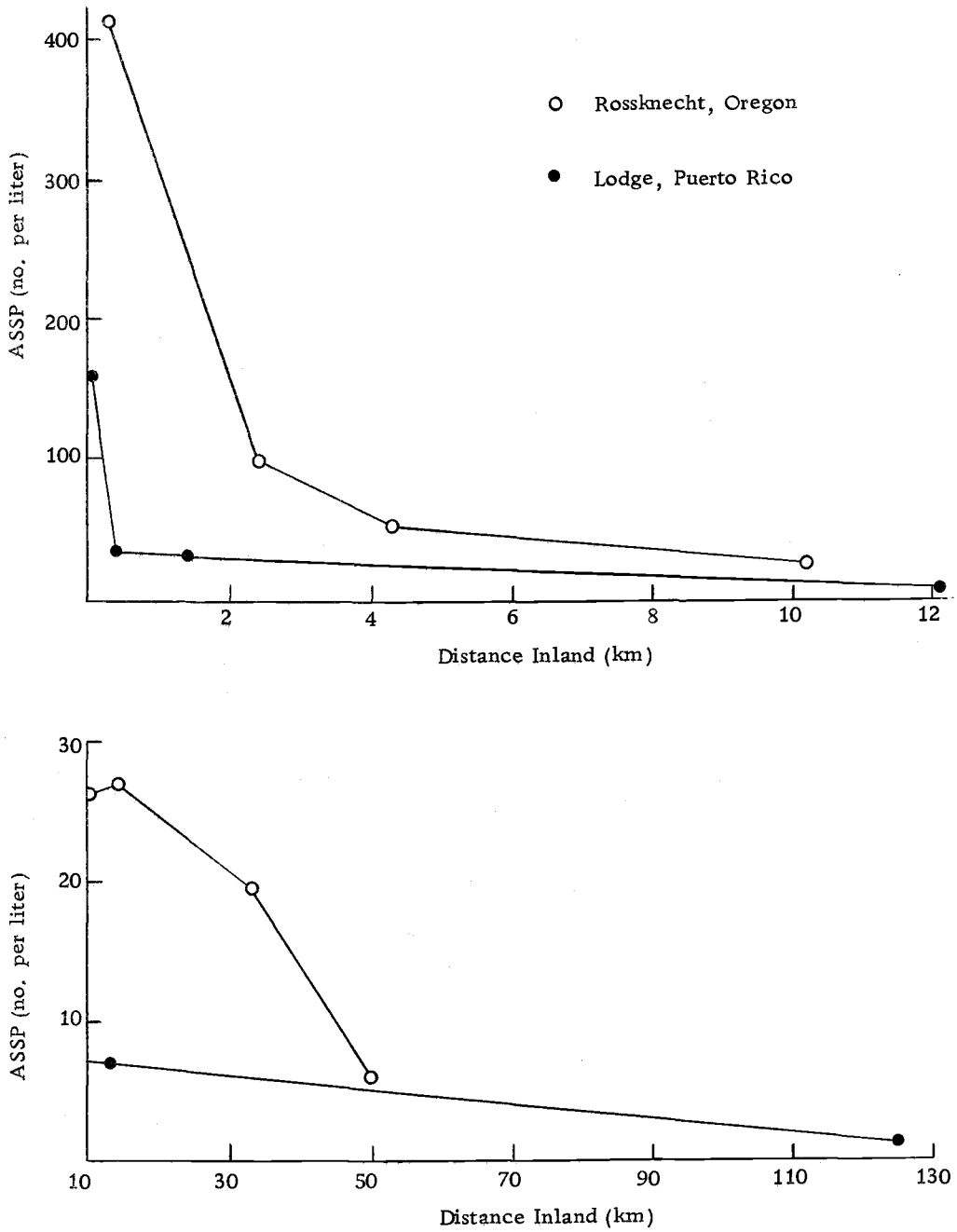

Figure 6.16. Data obtained by Lodge in Puerto Rico on ASSP with diameters $>3\mu$ Compared to similar data from this study.

VII. SUMMARY

The original objective was to determine the distribution of ASSP with distance inland from the ocean. To accomplish this, samples of ASSP were collected along an east-west line extending 50 km inland from Newport, Oregon. The sea-salt particles in the samples were counted and put into size classes according to their diameter. It was found that for samples collected at sea and greater than 8 km inland from the shoreline the relative frequency distribution of particle diameters was well-fitted by an exponential random variable. However samples collected inland within 8 km of the ocean had a size distribution significantly different from an exponential.

The size distribution data from samples collected at sea and greater than 8 km inland were fitted with a curve of the form $N_o/\alpha e^{-x/\alpha}$. Each sample had a different characteristic N_o and α. The fitting of these data with smooth exponential distribution functions aided in three ways:

(1) It smoothed the raw data which showed erratic fluctuations that were due to the sampling and counting procedure.

(2) It allowed estimates of particle number for size classes that were not counted and for size classes in which too few were counted to obtain an accurate distribution.

(3) It provided a distribution of mass curve from which an estimate of total mass of ASSP could be made.

For the data collected within 8 km of the beach the unsmoothed data was used in determining particle number and mass concentrations. Attempts were made to fit an exponential and a power law ($N(x) \propto x^{-\beta}$) to this data without success. The significantly different size distribution that was found in the region less than 8 km inland was attributed to the influence of the breaking waves and white water in the surf zone.

It was found that the amount of total mass and of particular sizes of ASSP decreases very sharply in the first 4 km inland from the shoreline, and further inland levels out and decreases more gradually. Typically, the total mass at 4 km inland was 15% of that at the coast and yet at 30 km inland there was a concentration about 8% of that at the coast. Several curves showing the observed distribution with distance inland are presented.

In addition to determining the inland distribution of ASSP it was found that the inland profiles of particular sizes of ASSP for the data collected July 14, 1971 could be fitted with a model developed by Toba and Tanaka to describe the inland distribution of ASSP. The fit to this model was good overall, but the fit was better for larger particles. The relatively poor fit to the smallest particles considered was attributed to the partial degeneration of these particles through the loss of chloride ion.

The good fit to the model for most of the particles is taken as an indication that the assumptions made by Toba and Tanaka concerning

the physical processes which determine the inland distribution are generally sound. There is a balance between particles supplied by advection and turbulent diffusive transport and particles lost by sedimentation and impaction on ground obstacles. The loss due to impaction on ground obstacles is apparently greater than the loss due to sedimentation.

The model is sensitive to relative humidity because of the growth of ASSP with increasing relative humidity. The sensitivity is greatest when the relative humidity gets above about 85 %. It would be better to sample ASSP when the humidity is low, because at high humidities a slight change in humidity will change the fall velocity of the particles, and the model for the inland distribution depends on the square of the fall velocity.

BIBLIOGRAPHY

Blanchard, D. C. and A. H. Woodcock. 1957. Bubble formation and modification in the sea and its meteorological significance. Tellus 9:145-158.

Bowen, E. G. 1950. The formation of rain by coalescence. Australian Journal of Scientific Research, ser. A, Physical Sciences 3:193-213.

Byers, H. R. 1965. Elements of cloud physics. Chicago, University of Chicago Press, 191 p.

Byers, H. R., J. R. Sievers and B. J. Tufts. 1957. Distribution in the atmosphere of certain particles capable of serving as condensation nuclei. In: Artificial stimulation of rain. London, Pergamon Press, 427 p.

Chapman, D. G. and D. S. Robson. 1960. The analysis of a catch curve. Biometrics 16:354-368.

Day, J. A. 1964. Production of droplets and salt nuclei by the bursting of air-bubble films. Royal Meteorological Society, Quarterly Journal 90:72-78.

Eriksson, Erik. 1959. The yearly circulation of chloride and sulfur in nature; meteorological, geochemical, and pedological implications. Part I. Tellus 2:375-403.

Eriksson, Erik. 1960. The yearly circulation of chloride and sulfur in nature; meteorological, geochemical, and pedological implications. Part II. Tellus 3:63-108.

Fletcher, N. H. 1966. The physics of rainclouds. Cambridge, Cambridge University Press, 390 p.

Hama, Kovichi and Noboru Takagi. 1970. Measurement of sea-salt particles on the coast under moderate winds. Papers in Meteorology and Geophysics 21:449-458.

Hogg, R. V. and A. T. Craig. 1968. Introduction to mathematical statistics. New York, Macmillan, 383 p.

Horne, R. A. 1969. Marine chemistry - the structure of water and the chemistry of the hydrosphere. New York. Wiley, 568 p.

Junge, C. E. 1953. Die Rolle der Aerosole und der gasförmigen Beimengungen der Luft im Spurenstoffhaushalt der Troposphäre. Tellus 5:1-26. (Abstracted in Meteorological Abstracts and Bibliography vol. 5, pt. 1:no. 5.1-105. 1954)

Junge, C. E. 1956. Recent investigations in air chemistry. Tellus 8:127-139.

Junge, C. E. 1963. Air chemistry and radioactivity. New York, Academic Press, 382 p.

Kientzler, C. F., A. B. Arons and D. C. Blanchard. 1953. Photographic investigation of the projection of droplets by bubbles bursting at a water surface. 11 numb. leaves. (Woods Hole Oceanographic Institution. Technical report no. 6 on Office of Naval Research Contract Nonr-798(00) Project NR 082-124)

Lodge, J. P. 1954. Analysis of micron-sized particles. Analytical Chemistry 26:1829-1831.

Lodge, J. P. 1955. A study of sea-salt particles over Puerto Rico. Journal of Meteorology 12:493-499.

Lodge, J. P. and B. J. Tufts. 1956. Techniques for the chemical identification of micron and submicron particles. Tellus 8:184-189.

Mason, B. J. 1962. Clouds, rain, and rain making. Cambridge, Cambridge University Press, 145 p.

Mészáros, Ernő. 1964. Repartition verticale de la concentration des particules de chlorures dans les basses couches de l'atmosphere. Journal De Recherches Atmosphériques, Jan./March 1964, p. 1-10. (Abstracted in Meteorological and Geoastrophysical Abstracts vol. 15, pt. 2:no. 15F-72. 1964)

Moore, D. J. and B. J. Mason. 1954. The concentration, size distribution and production rate of large salt nuclei over the oceans. Royal Meteorological Society, Quarterly Journal 80:583-590.

Murty, R. B. V., A. K. Roy and R. K. Kapoor. 1965. Aerosols at Delhi. In: Proceedings of the International Conference on Cloud Physics. Tokyo and Sapporo, 1965, p. 67-72.

Podzimek, Josef and Ivan Černoch. 1961. Hőhenverteilung der Konzentrationen von Riesenkernen aus Chloriden und Sulphaten. Geofisica Pura e Applicata 50:96-101. (Abstracted in Meteorological and Geoastrophysical Abstracts vol. 14, pt. 1:no. 14A-288. 1963)

Reitan, C. H. and R. R. Braham Jr. 1954. Observations of salt nuclei over the midwestern United States. Journal of Meteorology 11:503-506.

Roll, H. U. 1965. Physics of the marine atmosphere. New York, Academic Press, 426 p.

Seely, B. K. 1952. Detection of micron and submicron chloride particles. Analytical Chemistry 24:576-579.

Seely, B. K. 1955. Detection of certain ions in 10^{-10} to 10^{-15} gram particles. Analytical Chemistry 27:93-95.

Semonin, R. G. 1961. Atmospheric particulates in precipitation physics. 15 numb. leaves. (Illionis State Water Survey Meteorological Laboratory. Urbana, Illinois. Final report on National Science Foundation Grant no. G-6352)

Semonin, R. G. 1966. Observations of giant chloride particles in the Midwest. Journal de Recherches Atmosphériques, April/Sept. 1966, p. 251-260.

Squires, P. 1952. The growth of cloud drops by condensation. Australian Journal of Scientific Research, ser. A, Physical Sciences 5:59-86.

Tanaka, Masaaki. 1966. On the transport and distribution of giant sea-salt particles over land (I) theoretical model. Special Contributions of the Geophysical Institute, Kyoto University, December, 1966, p. 47-57.

Toba, Yoshiaki. 1965. On the giant sea-salt particles in the atmosphere. I. general features of the distribution. Tellus 17: 131-145.

Toba, Yoshiaki and Masaaki Tanaka. 1968. A continuous sampler for sea-salt particles especially of giant class and example of the analysis of data. Journal De Recherches Atmosphériques, Jan./June 1968, p. 79-85.

Tufts, B. J. 1959. Determination of micron-sized particles. Analytical Chemistry 31:242-243.

Twomey, S. 1954. The composition of hygroscopic particles in the atmosphere. Journal of Meteorology 11:334-338.

Twomey, S. 1955. The distribution of sea-salt nuclei in air over land. Journal of Meteorology 12:81-86.

Woodcock, A. H. 1950. Sea salt in a tropical storm. Journal of Meteorology 7:397-401.

Woodcock, A. H. 1952. Atmospheric salt particles and raindrops. Journal of Meteorology 9:200-212.

Woodcock, A. H. 1953. Salt nuclei in marine air as a function of altitude and wind force. Journal of Meteorology 10:362-371.

Woodcock, A. H. 1957. Atmospheric sea-salt nuclei data for project shower. Tellus 9:521-524.

Woodcock, A. H. and D. C. Blanchard. 1955. Tests of the salt-nuclei hypothesis of rain formation. Tellus 8:437-448.

Woodcock, A. H. and M. M. Gifford. 1949. Sampling atmospheric sea-salt nuclei over the ocean. Journal of Marine Research 8:177-197.

Woodcock, A. H. et al. 1953. Giant condensation nuclei from bursting bubbles. Nature 172:1144-1145.

APPENDIX

APPENDIX A

The α's and N_0's (defined in Chapter V) for the exponential size distributions fitted to the data from out at sea and from greater than eight kilometers inland were found by the maximum likelihood method. For a general discussion of the maximum likelihood method see, for example, Hogg and Craig (1968), Chapter 9. Chapman and Robson (1960) derive maximum likelihood estimators for a similar exponential distribution.

To obtain $\hat{\alpha}$ and $\hat{N}_0$ in this case, let $M_0, M_1, M_2, \cdots, M_k$ be the observed class frequencies where M_0 is the frequency of particles between 0 and 1.237 and is unknown. (M_1 is the number of particles observed in diameter class 1, M_2 the number in class 2, etc.) Let

$$N_0 = M_0 + M_1 + M_2 + \cdots$$

and

$$N = M_1 + M_2 + \cdots = N_0 - M_0 .$$

N is known but N_0 is not known, since M_0 is not observable.

The probabilities of occurrence of a randomly selected particle in the various diameter classes are:

$$P_0 = 1 - e^{-x_1/\alpha} = 1 - p^{\nu}$$

$$P_1 = e^{-x_1/\alpha} - e^{-x_2/\alpha} = p^{\nu}(1 - p)$$

$$P_2 = e^{-x_2/\alpha} - e^{-x_3/\alpha} = p^{\nu+1}(1 - p)$$

$$\vdots$$

$$P_k = e^{-x_k/\alpha} - e^{-x_{k+1}/\alpha} = p^{\nu+k-1}(1 - p)$$

where $p = e^{-h/\alpha}$ and $\nu = e^{x_1/h}$.

The frequencies $M_1, M_2, \cdots$ satisfy the definition of a multinomial random variable if N_0, the number of repeated independent multinomial trials is given. Given N_0, the conditional multinomial distribution has probability function

$$(A.1) \quad P_r\{M_1, M_2, \cdots, | N_0\} = \frac{N_0!}{(N_0 - N)! \prod_{k=1}^{\infty} M_k!} \left\{ \prod_{i=0}^{\infty} p_i^{M_i} \right\}$$

where $M_0 = N_0 - N$.

Substituting the diameter class probabilities into equation (A.1) and rearranging gives

$$(A.2) \quad P_r\{M_1, M_2, \cdots | N_0, p\} = \frac{N_0!}{(N_0 - N)! \prod_{k=1}^{\infty} M_k!} (1-p^{\nu})^{N_0 - N} (1-p)^N p^{\nu N+S}$$

where $$N = M_1 + M_2 + M_3 + \cdots = \sum_{i=1}^{\infty} M_i$$

and $$S = 0M_1 + 1M_2 + 2M_3 + \cdots = \sum_{i=1}^{\infty} (i-1)\, M_i .$$

From this it is clear that the statistics N and S are jointly sufficient for the estimation of N_0 and p.

In this case the probability function of $M_1, M_2, \cdots$ is also the likelihood function for N_0 and p. The maximum likelihood estimates of N_0 and p are those values, $\hat{N}_0$ and $\hat{p}$, which maximize the likelihood function. As is the usual practice we take the logarithm of the likelihood function (P_r) and maximize that:

$$L(N_0, p) = \log \{P_r(M_1, M_2 \cdots \mid N_0, p)\}$$

$$= -\log \prod_{k=1}^{\infty} M_k + \log \frac{N_0!}{(N_0-N)!} + (N_0-N)\log(1-p^{\nu})$$

$$+ N\log(1-p) + (\nu N + S)\log p$$

(Note: $$\frac{N_0!}{(N_0-N)} = \prod_{j=N_0-N+1}^{N_0} (j) \quad , \quad \text{so}$$

$$\log \frac{N_0!}{(N_0-N)} = \sum_{j=N_0-N+1}^{N_0} \log(j) \cong \int_{N_0-N}^{N_0} \log x \, dx \quad)$$

$$L(N_0, p) = -\log \prod_{k=1}^{\infty} M_i + \int_{N_0-N}^{N_0} \log x \, dx + (N_0-N)\log(1-p^{\nu})$$

$$+ (N\nu + S)\log p + N\log(1-p)$$

First we maximize L with respect to N_0:

$$\frac{\partial L}{\partial N}(N_0, p) = \log N_0 - \log(N_0-N) + \log(1-p^{\nu}) = 0$$

$$\log\left(\frac{N_0-N}{N_0}\right) = \log(1-p^{\nu})$$

$$\frac{N}{N_0} = p^{\nu} \rightarrow \hat{N}_0 = N\hat{p}^{-\nu}$$

Now, we maximize L with respect to p:

$$L(\hat{N}_0, p) = \int_{N(p^{-\nu}-1)}^{Np^{-\nu}} \log x \, dx + N(p^{-\nu}-1)\log(1-p^{\nu})$$

$$+ (N\nu + S)\log p + N\log(1-p)$$

$$\frac{\partial L}{\partial P}(\hat{N}_0, p) = [\log Np^{-\nu} - \log N(p^{-\nu}-1)](-\nu Np^{-\nu-1})$$

$$- N\nu p^{-\nu-1}\log(1-p^{\nu}) - \frac{N(p^{-\nu}-1)\nu p^{\nu-1}}{(1-p^{\nu})}$$

$$+ \frac{N\nu + S}{p} - \frac{N}{1-p} = 0 \quad .$$

Solving for p we find $\hat{p} = \frac{1}{1+N/S}$ and so $\hat{\alpha} = \frac{-h}{\log \hat{p}} = \frac{h}{\log(1+N/S)}$.

This is the maximum likelihood estimate of α that was used in the text. The estimate of N_0 is then:

$$\hat{N}_0 = N\hat{p}^{-\nu} = N\left(\frac{1}{1+N/S}\right)^{-x_1/h} = N\left(1+\frac{N}{S}\right)^{x_1/h}$$